REPUBLIC OF TÜRKİYE
YILDIZ TECHNICAL UNIVERSITY
GRADUATE SCHOOL OF SCIENCE AND ENGINEERING

DEVELOPMENT OF BIOSENSOR SURFACES FOR LIVER CANCER DETECTION

Muhammet GYLYJOV

MASTER OF SCIENCE THESIS

Department of Bioengineering

Program of Bioengineering

Supervisor

Prof. Dr. Cem Bülent ÜSTÜNDAĞ

Co-Supervisor

Dr. Özgür YILMAZ

August, 2024

REPUBLIC OF TÜRKİYE

YILDIZ TECHNICAL UNIVERSITY

GRADUATE SCHOOL OF SCIENCE AND ENGINEERING

DEVELOPMENT OF BIOSENSOR SURFACES FOR LIVER CANCER DETECTION

A thesis submitted by Muhammet GYLYJOV in partial fulfillment of the requirements for the degree of **MASTER OF SCIENCE** is approved by the committee on 08.08.2024 in Department of Bioengineering , Program of Bioengineering

Prof. Dr. Cem Bülent ÜSTÜNDAĞ
Yıldız Technical University
Supervisor

Dr. Özgür YILMAZ
TÜBİTAK Marmara Research Center
Co-supervisor

Approved By the Examining Committee

Prof. Dr. Cem Bülent ÜSTÜNDAĞ, Supervisor
Yildiz Technical University _____

Assoc. Prof. Dr. Azime ERARSLAN, Member
Yildiz Technical University _____

Asst. Prof. Dr. Songül ULAĞ, Member
Marmara University _____

I hereby declare that I have obtained the required legal permissions during data collection and exploitation procedures, that I have made the in-text citations and cited the references properly, that I haven't falsified and/or fabricated research data and results of the study and that I have abided by the principles of the scientific research and ethics during my Thesis Study under the title of "Development of Biosensor Surfaces for Liver Cancer Detection" supervised by my supervisor, Prof. Dr. Cem Bülent ÜSTÜNDAĞ and co-supervisor Dr. Özgür YILMAZ. In the case of a discovery of false statement, I am to acknowledge any legal consequence.

Muhammet GYLYJOV

Signature

This work was supported by the Scientific and Technological Research Council of Türkiye (TÜBİTAK) Grant No: 20AG012

Dedicated to my family

and friends

ACKNOWLEDGEMENTS

First of all, I would like to express my gratitude towards my supervisors Prof. Dr. Cem Bülent ÜSTÜNDAĞ and Dr. Özgür YILMAZ for their help, motivation, patience and knowledge. Their guidance enabled me to do my research and helped me to boost my knowledge in my sphere of interest. I would also like to thank Dr. Sevgi GÜLYÜZ and the medicinal chemistry team, Assoc. Prof. Dr. İlke GÜROL and her team, Dr. Sefer BADAY, Muhammed Esad KALAYCI, Ayşenur ARSLAN, Kübra ARANCI ÇİFTÇİ, Sümeyra AYAN, Sema Nur YILDIRIM, Zehra Beyza ALBORU, Zehra Elif AYDIN and Canan Buse ABDUL, who were in the project with me, for their help.

I would also like to thank Dr. Esin AKÇAEL and her team Dr. İlkay Göksu POLAT, Dr. Göknur Gizem DİNÇ, Sümeyye ULUBAY, Pelin Su KESKİNBURUN and Prof. Dr. Hüseyin KIZIL and his team for their aid in the project and wisdom.

Finally I would like to thank my family; my mother, aunt, brother, cousin, grandfather, deceased grandmother, uncles in law, and extended family whose support were present my whole and without whom I would not be here writing this thesis.

I would also thank the Scientific and Technological Research Council of Türkiye (TÜBİTAK) (Project name: Development of sensing components for cancer diagnosis and validation of ıntegrated diagnostic systems, Project number: 20AG012) for their valuable support.

Muhammet GYLYJOV

TABLE OF CONTENTS

LIST OF SYMBOLS

amu	Atomic Mass Unit
°C	Celsius
µg	Microgram
µl	Microliter
µm	Micrometer
mg	Milligram
ml	Milliliter
mm	Millimeter
mM	Millimolar
min	Minute
nm	Nanometer
%	Percent
v	Volume

LIST OF ABBREVIATIONS

AFP	Alpha fetoprotein
BCA	Bicinchoninic acid
BMI	Body Mass Index
CDR	Complementarity Determining Region
CE	Counter Electrode
CEA	Carcinoembryonic Antigen
CT	Computed Tomography
CV	Cyclic Voltammetry
DCP	Des-γ-Carboxy Prothrombin
DIEA	N,N-Diisopropylethylamine
DMF	Dimethyl Formamide
DNA	Deoxyribose Nucleic Acid
EDC	N-(3-Dimethylaminopropyl)-N-Ethylcarbodiimide Hydrochloride
Fmoc	Fluorenylmethyloxycarbonyl Protecting Group
FRET	Fluorescence Resonance Energy Transfer
HBTU	Hexafluorophosphate Benzotriazole Tetramethyl Uronium
HCC	Hepatocellular Carcinoma
HPLC	High-Performance Liquid Chromatography
LC/MS	Liquid Chromatography/Mass Spectroscopy
LT	Liver Transplant
mAb	Monoclonal Antibody
MELISA	Magnetic Bead-Based Enzyme Linked Immunoassay
MMB	Magnetic Microbeads
MRI	Magnetic Resonance Imaging
MUA	Mercaptoundecanoic Acid
MWA	Microwave Ablation
NHS	N-Hydroxysuccinimide
OLT	Orthotopic Liver Transplantation
PBS	Phosphate Buffered Saline
RE	Reference Electrode
SPPS	Solid-Phase Peptide Synthesis
SPR	Surface Plasmon Resonance

TACE	Transarterial Chemoembolization
TARE	Transarterial Radiation
TFA	Trifluoracetic Acid
TIPS	Triisopropylsilane
WE	Working Electrode
UNAM	Bilkent University National Nanotechnology Research Center
UV	Ultraviolet

LIST OF FIGURES

LIST OF TABLES

ABSTRACT

Development of Biosensor Surfaces for Liver Cancer Detection

Muhammet GYLYJOV

Department of Bioengineering
Master of Science Thesis

Supervisor: Prof. Dr. Cem Bülent ÜSTÜNDAĞ
Co-supervisor: Dr. Özgür YILMAZ

Hepatocellular Carcinoma (HCC) is one of the biggest causes of cancer related death worldwide. HCC is generally caused by acute or sub-acute injuries caused by Hepatitis B, C that proceed into cirrhosis. Early detection of HCC is very crucial for patient survival and several biomarkers have been discovered for HCC detection. There are several biomarkers for specific HCC detection such as alpha-fetoprotein (AFP), des-γ-carboxy prothrombin (DCP) and glypican-3. Among those biomarkers AFP is the most researched biomarker. However, AFP has low sensitivity, especially in the early stages of the disease. Studies have shown that AFP frequently fails to detect early-stage HCC, resulting in reliable results largely in later stages when the tumor burden is higher.

In this thesis, it is hypothesized that the usage of peptides can increase sensitivity of AFP biosensors. Antibody-like peptides bind to their target with high selectivity and selectivity. Peptides are simpler in structure, smaller, and can withstand a wider range of environmental changes such as pH and temperature. This thesis focuses on the peptide sequences derived from Complementarity Determining Region (CDR) of human anti-AFP antibody and their chemical immobilization into various surfaces for later use in HCC biosensors. The peptides were synthesized using solid-phase peptide synthesis methods and immobilized on magnetic microbeads and

gold surface. Synthesized SYVIH and YTSALLP peptides had high purity of %95.4 and %96.9 respectively. The optimal binding capacity of SYVIH and YTSALLP peptides on magnetic microbeads was found to be 52 mg and 59.8 mg per milligram of beads. CV results of SYVIH peptides immobilized on gold electrodes were measured as 4.4 mA and addition of AFP protein decreased the current signal to 3.04 mA. This methodological approach aims to improve the sensitivity and specificity of biosensors with AFP biomarker, potentially improving the detection and monitoring of HCC.

Keywords: Alpha-fetoprotein, biosensor, hepatocellular carcinoma, peptide, solid-phase peptide synthesis

ÖZET

Karaciğer Kanseri Tespitine Yönelik Biyosensör Yüzeylerinin Geliştirilmesi

Muhammet GYLYJOV

Biyomühendislik Anabilim Dalı
Yüksek Lisan Tezi

Danışman: Prof. Dr. Cem Bülent ÜSTÜNDAĞ
Dr. Özgür YILMAZ
Eş-Danışman: Dr. Özgür YILMAZ

Hepatoselüler Karsinom (HSK), dünya çapında kansere bağlı ölümlerin en büyük nedenlerinden biridir. HSK genellikle Hepatit B ve Hepatit C'nin neden olduğu ve siroza dönüşen akut veya sub-akut hasarlardan kaynaklanır. HSK'nın erken teşhisi, hasta için hayati önem arz etmektedir ve HSK'nın teşhisi için çeşitli biyobelirteçler keşfedilmiştir. Alfa-fetoprotein (AFP), des-γ-karboksi protrombin (DCP) ve glikan-3 gibi çeşitli biyobelirteçler HSK'nın teşhisi için keşfedilen biyobelirteçlerden bazılarıdır ve biyobelirteçler arasında AFP en çok çalışılan biyobelirteçtir. Ancak AFP, özellikle hastalığın erken evrelerinde düşük spesifiteye sahiptir. Önceki çalışmalar AFP'yi tespit etme yöntemlerinin HSK'nın erken evrelerinde hastalığı saptamada sıklıkta başarısız olduğunu ve büyük ölçüde tümörün daha tehlikeli olduğu sonraki evrelerde güvenilir sonuçlar verdiğini göstermiştir.

Bu tezde, peptitlerin kullanımının AFP biyosensörlerinin hassasiyetini artırabileceği varsayılmaktadır. Peptitler antikorlara ziyade yapı olarak daha basit, daha küçük ve pH, sıcaklık gibi çevresel değişikliklere daha dayanıklıdır. Bu tez, insan anti-AFP antikorunun tamamlayıcılık belirleme bölgesinden (CDR) türetilen peptit dizilerin sentezine ve sentezlenen peptitlerin daha sonra HSK biyosensörlerinde kullanılmak üzere çeşitli yüzeylere kimyasal olarak

immobilizasyonuna odaklanmaktadır. Peptitler katı faz peptit sentezi yöntemini kullanılarak sentezlenerek manyetik mikroboncuklara ve altın yüzeye immobilize edilmişlerdir. SYVIH ve YTSALLP peptidleri sırasıyla %95,4 ve %96,9 yüksek saflık oranında sentezlenmiştir. SYVIH ve YTSALLP peptitlerinin manyetik mikroboncuklar üzerindeki optimum bağlanma kapasitesi bir miligram boncuk başına 52 mg ve 59.8 mg olarak bulunmuştur. Altın elektrotlara immobilize edilen SYVIH peptitlerinin CV sonuçları 4.4 mA olarak ölçülmüş ve AFP proteini ilavesi akım sinyalini 3.04 mA'e düşürmüştür. Bu metodolojik yaklaşım, AFP biyobelirteçli biyosensörlerin duyarlılığını ve özgüllüğünü artırarak HSK'nin tespitini potansiyel olarak geliştirmeyi amaçlamaktadır.

Anahtar Kelimeler: Alfa-fetoprotein, biyosensör, hepatosellüler karsinom, katı faz peptit sentezi, peptit

1
INTRODUCTION

1.1 Literature Review

Hepatocellular carcinoma (HCC) has one of the highest mortality rates among cancer types. According to GLOBOCAN 2022 data there are 866 thousand incidents and 758 thousand deaths worldwide in 2022, making it the third deadliest cancer type [1]. HCC is the last stage of event chains that consist of tissue inflammation, fibrosis and cirrhosis. Cirrhosis, Hepatitis B and C viruses, diabetes and non-alcoholic fatty liver disease pose great risk for HCC development [2]. Unfortunately, the diagnosis of HCC is mostly given in the last stages of cancer making the treatment more challenging. Early detection of HCC is very important with treatment success varying from 30-50% while in the late stages of the disease the treatment success drops significantly [3].

There are several biomarkers for the detection of HCC such as alpha-fetoprotein (AFP), des-γ-carboxy prothrombin (DCP) and glypican-3. Among those molecules AFP is the most widely studied one [4]. AFP is a 70 kDa protein produced in a yolk sac and fetal liver during fetal development [5]. AFP plays a huge role in the development of HCC by blocking apoptotic signals and suppressing immune response in the human body [6], [7]. Unfortunately, in the early stages AFP as a biomarker isn't very reliable due to low sensitivity. Studies have shown that AFP shows reliable results largely in later stages when the tumor burden is higher [8], [9].

Magnetic microbeads are spherical molecules that usually consist of iron or nickel core with surface modifications. Magnetic beads are widely used in nucleic acid purification and separation [10]. Due to lack of chemical waste, magnetic microbeads are more appealing compared to traditional separation techniques. This property also makes them a great candidate for ligand immobilization for biosensor surfaces. Magnetic beads can be easily manipulated through external magnets that can immobilize the ligand without extra chemicals [11].

Biosensors are devices that quantitively or qualitatively detect the metabolic processes and/or target biomolecules in a living organism. Biosensors use a bioreceptor on the sensor surface to recognize a target analyte and generate a signal (eg. optical, electrochemical, acoustic). This signal is then converted and displayed by a processor. Biosensors have gained popularity in biomedical applications due to the need for noninvasive, sensitive, and accurate detection systems [12], [13].

Peptides, biomolecules consisting of several amino acid chains, are involved in many physiological and metabolic activities in the human organism. They play key roles in transporting and intercellular communication [14],[15]. Antibody-like peptides are widely used in biotechnology and medical fields. Peptides are simpler in structure, can be easily modified, more stable and can achieve higher sensitivity and selectivity than antibodies. Additionally, the synthesis of peptides is much simpler than antibodies which makes them more appealing in the scientific field [16], [17].

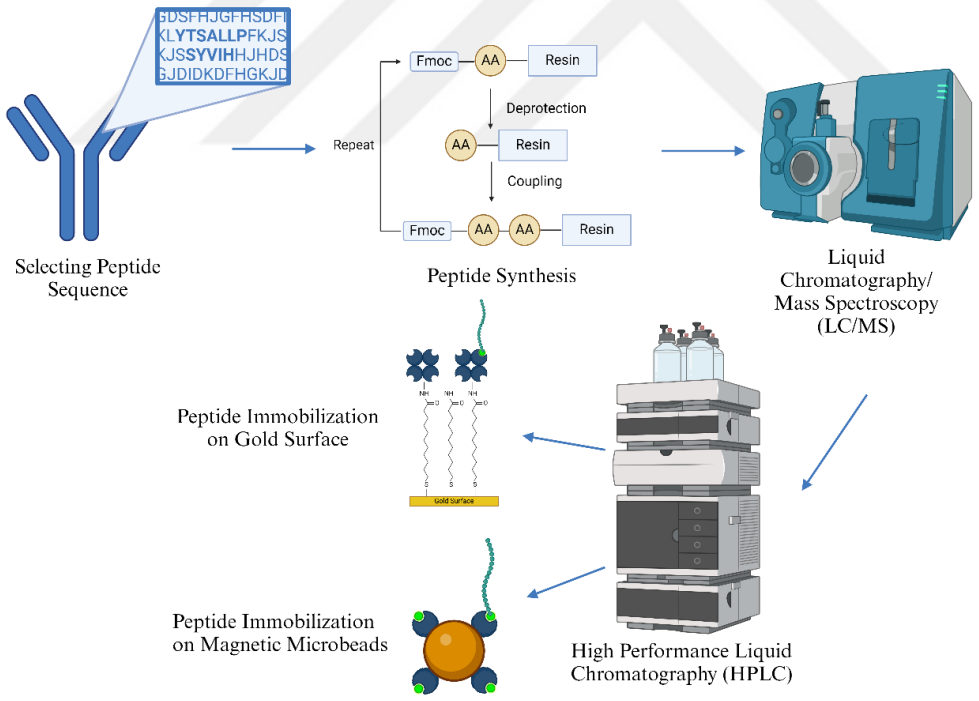

Figure 1.1 Schematic representation of peptide synthesis and their immobilization steps

1.2 Objective of the Thesis

The objective of this thesis is to synthesize, purify, and characterize peptides derived from the complementarity determining region (CDR) region of the human anti-AFP antibody, designed by HPEPDOCK for AFP detection. The peptides synthesized by solid-phase peptide synthesis (SPPS) method were then immobilized on magnetic microbeads and gold surface for further biosensor applications (eg. Magnetic bead-based enzyme linked immunosorbent assay (MELISA), microfluidics). The widespread impact of this thesis is to develop a peptide-based biosensor surfaces which are capable of binding to AFP with high selectivity and sensitivity.

1.3 Hypothesis

The hypothesis of this thesis is to synthesize, purify, characterize peptides that show affinity towards AFP molecule and immobilize them into magnetic microbeads and gold surface. Peptide usage will increase the sensitivity and selectivity for AFP targeting and enable the production of more affordable and more durable biosensor surfaces. As a result of this thesis, preliminary studies will be carried out to develop biosensor surfaces with AFP-specific peptides.

2
GENERAL INFORMATION

2.1 Hepatocellular Carcinoma

Hepatocellular carcinoma (HCC) is one of the leading causes of cancer-related deaths worldwide. According to GLOBOCAN 2022 data (Figure 1.1) there have been over 758 thousand recorded deaths worldwide from liver cancer making it the third deadliest cancer [1]. The number of people with HCC varies throughout countries and can be attributed to different risk factors present in various countries. Hepatitis B and C infections pose great risk for the development of HCC [18]. HCC is generally caused by acute or sub-acute injuries in the liver that develop into fibrosis and cirrhosis. HCC development without preexisting cirrhosis is observed less frequently. HCC is the final stage of a progressive hepatic carcinogenesis sequence, starting with regenerative nodules, dysplastic nodules and evolving into HCC [19]. The treatment and management of HCC is complicated due to treatment resistance high chance of recurrence. Early forms of HCC can be treated with surgical operations such as liver resections. Chemotherapy and immunotherapy are required to treat advanced stages of HCC [20].

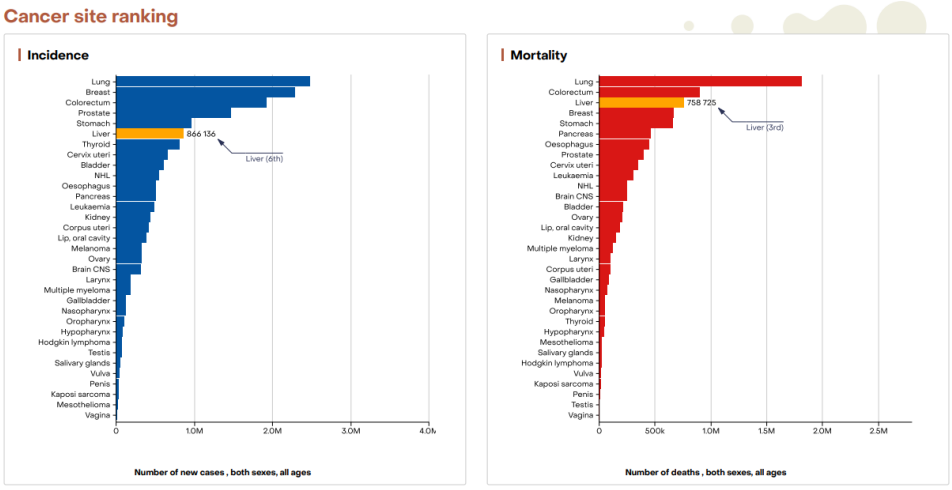

Figure2.1 Incidence and mortality rates of different cancer types worldwide [1]

2.1.1 Risk Factors

Cirrhosis and chronic liver disease are the most prominent risk factors for the development of HCC, with excessive alcohol consumption and viral hepatitis being

the major global risk factors. Diabetes mellitus has a direct impact on the liver since it plays an important part in the metabolism of glucose. Diabetes can cause chronic hepatitis, fatty liver, liver failure, and cirrhosis which can further develop into HCC [21]. Another health factor regarding HCC is obesity, which is associated with a variety of hepatobiliary diseases. The relative risk of HCC is 117% for overweight individuals and 189% for obese individuals. Another factor that can influence HCC development is the sex of an individual, with males having a higher likelihood of HCC with the ratio of 2:1-4:1. This increase in the likelihood can be associated with higher indulgence in alcohol and tobacco, and males having higher body mass index (BMI) than females. Additionally, males have a higher chance of being infected by hepatitis [22], [23].

2.1.2 Diagnosis

Early diagnosis of HCC is key for successful treatment of the disease. Various imaging devices such as magnetic resonance image (MRI) and computer tomography (CT) is used to detect abnormalities in the human liver. A recent meta-analysis of the diagnostic performance of CT and MRI for assessing HCC indicated that MRI has a greater per-lesion sensitivity than multidetector CT and should be the preferable imaging modality for the detection of HCC in patients with chronic liver disease. If the diagnosis is still questionable, a serum AFP level of more than 400 ng/ml has a significant positive predictive value. Percutaneous biopsy should only be performed on nodules that are radiologically abnormal on CT or MRI for HCC [24], [25].

2.1.3 Pathophysiology of HCC

Pathophysiology of HCC includes the accumulation of genetic alterations in pre-neoplastic hepatocytes, which result in malignant tumor formation that can appear as single of multiple lesions [26]. The liver lobule contains hepatocytes, cholangiocytes, and non-parenchymal cells such as Kupffer cells and hepatic stellate cells (HSCs). Toxin exposure and immunological responses can stimulate Kupffer cells and HSCs, resulting in inflammation and necrosis [27]. This process can result in liver fibrosis and cirrhosis, affecting blood flow and increasing the risk of liver failure.

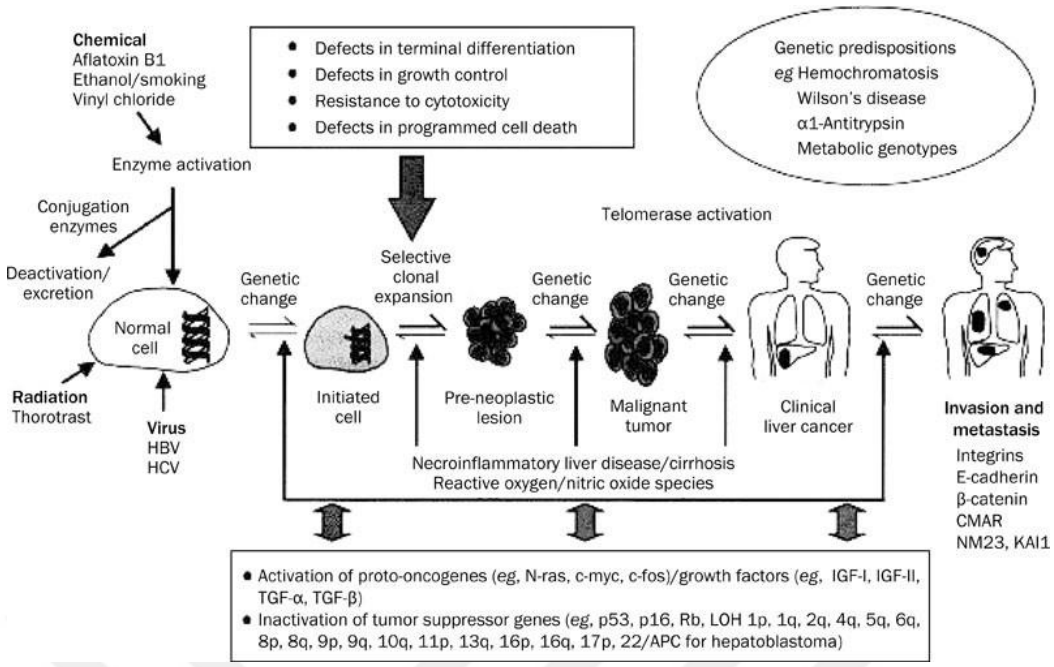

Figure2.2 Schematic representation of HCC carcinogenesis [28]

The tissue environment is crucial for tumor formation and growth. The tumor stroma consists of fibroblasts, macrophages (such as liver resident Kupffer cells and other tumor-infiltrating cells), leukocytes, hepatic stellate cells (HSCs), endothelial cells, pericytes, neutrophils, and dendritic cells [29]. Each of these cells generates growth factors, cytokines, chemokines, free radicals, and other tumorigenic substrates that aid in tumor development and progression.

Cancer-associated fibroblasts and dendritic cells are crucial in tumor-stromal interactions and tumor immune survelience in HCC and other cancers. Cancer-assosiated fibroblasts produce crucial cytokines and growth factors for the development of tumors such as epidermal growth factor (EGF), hepatocyte growth factor (HGF), fibroblast growth factor (FGF), interleukin 6 [30]. Dendritic cells process antigens and present them to invading cytotoxic T lymphocytes, which can reduce recurrence of HCC. HBV-encoded X protein and HCV non-structural proteins promote HSC activation and proliferation,which can the develop into cancer-associated fibroblasts in response to liver injury. Hypoxia promotes HCC proliferation, angiogenesis, metastasis, and chemo- and radioresistance [31].

2.1.4 Treatment

Unfortunately, HCC is frequently diagnosed after patients have developed symptoms and some degree of liver dysfunction. At this point, there is hardly any

effective medication that can enhance survival. Additionally, the morbidity associated with treatment methods is high. Currently, there are various surgical and nonsurgical treatment methods available that can improve survival rates. The best results are obtained when patients are appropriately chosen for each treatment option. To have the best possible outcome, patients with HCC must receive a multidisciplinary approach, regardless of the treatment method [32], [33].

Table2.1 Summary of results of studies in the management of early HCC [3]

HCC stage	Treatment arms	Overall survival
Resection		
Early	HCC ≤5 cm, no portal hypertension	50–70%
	HCC >5 cm or portal hypertension	35–55%
Liver transplantation		
Early	Milan	70–80%
Early or intermediate	Down-staged	60–70%
Ablation		
Early	Radiofrequency ablation	70%
	Percutaneous ethanol injection	60%
	Microwave ablation	65%
	Cryoablation	40%

Table2.2 Summary of results of studies in the management of intermediate and advanced HCC [3]

HCC stage	Treatment arms	Overall survival (months)
Transarterial therapies		
Intermediate	TACE	26–32
	TACE plus brivanib	26
	TACE plus sorafenib	21
	TACE plus orantinib	31
	TACE plus sorafenib	13
Transarterial radioembolization		
Advanced	TARE	8–9
	TARE plus sorafenib	12

Surgical treatment of HCC includes resection and liver transplant. Resection is described by removing a part of the liver. Patients with a single tumor restricted to the liver, no radiologic signs of vascular invasion, and normal liver function qualify for this treatment. Surgical resection is the preferred treatment for noncirrhotic

individuals and has the highest cure rate [34]. Orthotopic liver transplantation is the most effective cure for individuals with decompensated cirrhosis, and HCC is the only solid cancer that can be treated with transplantation [35].

Nonsurgical treatments include transarterial chemoembolization (TACE), transarterial radiation (TARE) and microwave ablation. TACE treatment consists of administering a highly concentrated dosage of chemotherapeutic drugs via selective catheterization of the tumor feeding arterial branch. The embolization of the tumor microcirculation after infusion prolongs cytotoxic effect, reducing the systemic toxicity of chemotherapy in patients [36]. TARE using Yttrium-90 (Y90) is an increasing area of study because of its advantages in early, middle, and late-stage hepatocellular carcinoma. The treatment method and dosimetry goals are determined by treatment aim, which includes curative therapy, bridge to transplant, and disease downstaging [37].

2.2 Alpha-Fetoprotein (AFP)

The most common biomarker of HCC is Alpha-fetoprotein. AFP is 70 kDa protein produced in a yolk sac and fetal liver during fetal development. It is assumed to be a fetal version of serum albumin that transports fatty acids and cells. AFP is available in monomeric, dimeric, and trimeric forms [5]. Bergstrand and Czar discovered AFP in human fetal sera in 1956. It functions as a transporter for a variety of ligands, including bilirubin, fatty acids, and possibly some medicines. Its levels often fall significantly after birth and stay low for the rest of life [38]. Since its discovery as an oncofetal biomarker, it has been utilized for HCC screening, diagnosis, prognosis, and treatment evaluation. Furthermore, it serves as an indicator in some new criteria for selecting liver transplant beneficiaries. Over the last decade, there has been some advancement in the use of AFP based on clinical and basic research [39]. In addition to being a biomarker for HCC and liver transplant, it could be used for immune treatment and to define HCC molecular classes. However, even if a low-level cutoff is used (10–20 ng/mL), the sensitivity value of AFP is around 60% and the specificity is still inadequate. Furthermore, serum AFP levels remain normal in 15–30% patients with advanced HCC [9]. To combat these drawbacks several strategies were utilized.

Figure 2.3 3D structure of AFP [40]

AFP blocks the transmission of apoptotic signals and inhibits apoptosis. AFP interacts directly with the amino acid residues Glu-248, Asp-253, and His257 of loop-4 of caspase-3 molecules in the cytoplasm, inhibiting the caspases signaling cascade and preventing tumor necrosis factor-related apoptosis-inducing ligand (TRAIL) and other leukocyte-secreted molecules from inducing apoptosis in HCC cells [6]. Research also found that AFP activates the PI3K/ AKT signaling pathway that stimulates the expression of proliferation-related oncogenes and metastasis-related genes [7]. Furthermore, AFP suppresses immune function by inhibiting lymphocyte and macrophage function which aids HCC cells to evade immune cells and survive to metastasis stage [41].

2.3 Antibody

Antibodies are Y shaped proteins secreted by B cells that selectively bind to their target proteins (antigens). There are two types of antibodies depending on their selectivity. Monoclonal antibodies bind only to one specific antigen while polyclonal antibodies can bind to a family of antigens. The high affinity of antibodies towards antigens makes them a promising candidate for biosensors and drug applications. Antibodies have been utilized in cancer detection and treatment. Monoclonal antibodies (mAbs) can kill tumor cells by direct action (for example, receptor blockage), immune-mediated cell death mechanisms, payload delivery, and antibody-specific effects on the tumor vasculature and stromal cells [42], [43]. To overcome the shortcomings of antibody new detection molecules for biosensor surfaces such as aptamers and peptides have been designed.

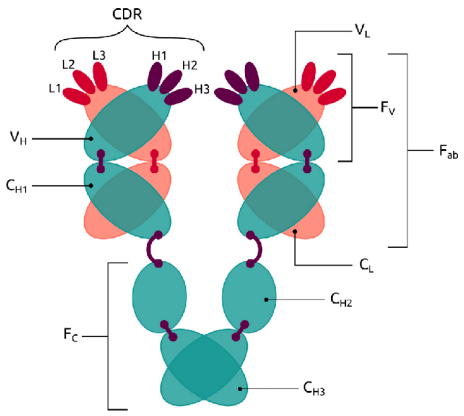

Figure 2.4 Schematic representation of a structure of an antibody [44]

2.3.1 Aptamers

Aptamers are small oligonucleotide or peptide molecules that act like antibodies that bind to their target with high affinity. Unless explicitly stated otherwise, aptamer refers to nucleic acid aptamers. The name aptamer comes from the Latin words "aptus" (fitting) or "aptare" (to fit) and the Greek word "meros" meaning part [45]. Aptamers' ability to fold into or around the complex surfaces of a target molecule allows them to pick a wide range of targets, even those that other affinity reagents find difficult to bind. Aptamers can target peptides, proteins, metabolites, small organic compounds, carbohydrates, biological cofactors, metal ions, toxins, viruses, pathogenic bacteria and yeast, and mammalian cells [46]. Peptide aptamers have high affinity and selectivity to the protein it binds and can reduce the risk of false positive results. Additionally, peptides are chemically and thermally more stable making them durable for the environmental changes [47].

2.4 Solid-Phase Peptide Synthesis (SPPS)

Solid-phase peptide synthesis (SPPS) is a widely used method for the synthesis of peptides developed by Robert Bruce Merrifield in 1963 [48]. The principle of SPPS includes anchoring the peptide into a solid resin and growing by coupling the amino acids on N-terminal. SPPS has various advantages, such as high yield, simplicity of automation, and the capacity to rapidly synthesize complicated peptides and peptide libraries. However, it has limitations, including the possibility of incomplete reactions and difficulty in synthesizing long peptide chains due to aggregation or steric hindrance [49].

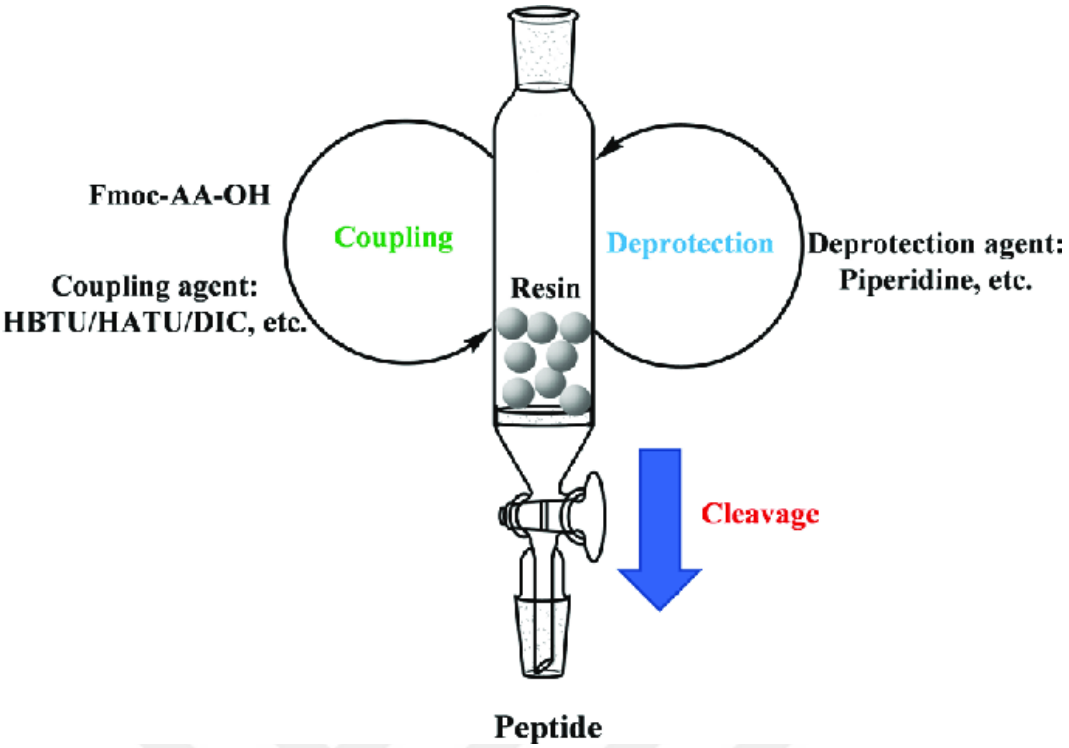

Figure 2.5 Schematic representation of SPPS procedure [50]

SPPS starts with covalently bonding the C-terminal of an amino acid onto a solid resin. After the first amino acid is anchored, the peptide chain is expanded using a series of coupling and deprotection steps. To prevent side reactions, the amino acids are coated at the N-terminus with a temporary protective group, such as fluorenylmethyloxycarbonyl (Fmoc). During each cycle, the deprotection group of each amino acid is removed, typically with piperidine, exposing the amine group. The next amino acid in the cycle is then activated by a coupling reagent such as hexafluorophosphate benzotriazole tetramethyl uronium (HBTU). The cycle is repeated until the last amino acid is added. Following the addition of the last amino acid, the peptide chain is then cleaved from the resin using trifluoroacetic acid (TFA). Finally, after synthesis the peptide undergoes characterization and purification steps, after which the finished peptide is ready to use [48], [51], [52],

2.5 Magnetic Beads

Magnetic beads are effective tools for purifying, detecting, and analyzing analytes from complex matrices. Magnetic beads' superparamagnetic properties make them suitable for a variety of analytical applications [53]. The beads typically consist of core and surface coating. The core of magnetic beads can be made from pure metals

(copper, iron, nickel), or metal oxides (iron oxide, copper oxide). Surface coating of the magnetic beads is typically made out of nonpolymeric stabilizers (alkanesulphonic and alkanephosphonic acids, lactobionic acid, lauric acid) or polymeric stabilizers (alginate, chitosan, dextran, polyethylene glycol) [54]

There are several applications of magnetic beads in the fields of biotechnology and medical diagnostics. One of the most widely used applications of magnetic beads is the purification of various biomolecules, especially nucleic acids. The usage of magnetic beads in the purification process offers possibility process automation, scalability and the capability to move particles form well to well and avoiding the cross-contamination [11]. Recently, Xu et al proposed a novel system for purification of DNA samples via external neodymium magnet in multi-laminar microfluidic environment.

Furthermore, magnetic beads are used in immunoassays by modifying their surface with various antibodies and aptamers. Magnetic beads can be easily manipulated with a magnet, their surface can be modified to increase specificity and sensitivity and have high surface-to volume-ratio. These qualities made magnetic beads attractive for biosensor applications. Huergo et al immobilized recombinant 6xHis-tagged SARS-CoV-2 Nucleocapsid protein on a nickel beads and conjugated with horse radish peroxidase thus making a magnetic-bead enzyme-linked immunosorbent assay (MELISA) [55].

2.6 Biosensor

Devices containing biological sensing elements in various fields of biomedicine, drug discovery, food safety are called biosensors. The first biosensor was invented by Clark and Lyons in 1962 for glucose measurement. This biosensor used the strategy of electrochemical detection of oxygen or hydrogen peroxide using a glucose oxidase electrode for glucose measurement. Since then, advances in electrochemistry, nanotechnology and bioelectronics have led to various developments in the application and construction of biosensors. Today's biosensors can generate a specific signal by modifying the surface with different components (enzyme, antibody, DNA, cell, aptamer) [13]

2.6.1 Optical Biosensors

Optical biosensors utilize light to detect target objects and the environment. Within the evanescent field, analytes are recognized by co-receptors fixed to the surface of a waveguide. Phase, amplitude, resonance momentum, changes corresponding to object concentration and biomolecular conformation can be evaluated. The refractive index changes with the addition of a biological sample. These changes in the refractive index enable the detection of the material at hand[56]. Optical biosensors have advantages such as high sensitivity, specificity, reliability and the potential to be integrated on a single chip [57]. Moreover, incorporation of nanomaterials like gold nanoparticles (AuNPs), quantum dots (QDs), and graphene oxide (GO) significantly enhances sensitivity and specificity of these types of biosensors. Optical biosensors can be classified as surface-plasmon resonance (SPR), fluorescence, luminescence, optical waveguide etc. [58].

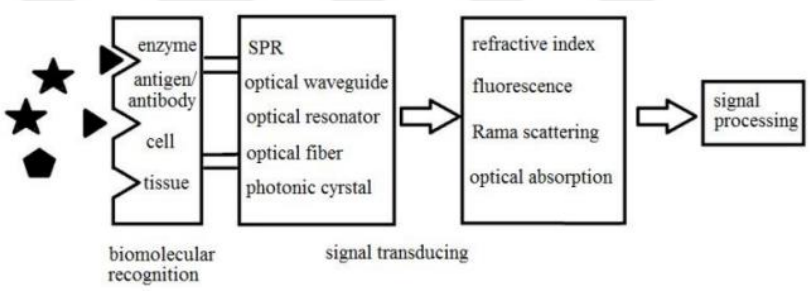

Figure 2.6 Schematic representation of components of an optical biosensor [56]

Surface Plasmon Resonance (SPR) Biosensors: Surface plasmon resonance (SPR) biosensors work on the principle that incoming light at a given angle induces surface plasmons, coherent oscillations of electrons at the interface between a metal and a dielectric (e.g., glass) substrate. When target molecules bind to antibodies or aptamers attached to a metal surface, the local refractive index changes. SPR is one of the most often utilized techniques in the field of on-the-spot detection of cancer biomarkers because of its non-destructive nature, rapid and real-time evaluation of the intended biomarker with great selectivity and repeatability [59], [60]. As an example, for SPR biosensor Wang et al employed the dual signal amplification strategy using AuNP-antibody and antibody-QD conjugates for increased sensitivity towards AFP, carcinoembryonic antigen (CEA) and cytokeratin fragment 21-1 [61].

Chemical Luminescence Biosensors: Chemical luminescence occurs when light is emitted from an exergonic chemical reaction that yields an intermediate in its singlet excited state, undergoing radiative decay. Several chemiluminescence-based biosensors have been developed for the quantitative multiplex analysis of organic molecules (hormones, drugs, etc.), proteins and nucleic acids. Huang et al developed a biosensor where AFP was sandwiched between gold immobilized primary antibody and HRP modified secondary antibody which utilized chemiluminescence for the detection of biomarker [62].

Fluorescence Biosensors: Fluorescence is the emission of photons by molecules after absorbing electromagnetic energy. Fluorescence is a great tool for bioanalysis that provides an understanding of biological mechanisms, structures and molecular interactions. Fluorescence biosensors can achieve sensitivity that reaches the level of a single molecule [63]. Several AFP biosensors were developed utilizing fluorescence as their detection method. Xu et al. developed a simple and sensitive biosensor utilizing fluorescence resonance energy transfer (FRET) for the simultaneous detection of multiple tumor target markers integrated by MoS2 nanosheets with multicolored gold nanoclusters [64]. Guo et al. developed biosensors for detection of cancer biomarkers of AFP and CEA using ZnO nanowire-integrated microfluidic devices [65].

2.6.2 Electrochemical Biosensors

Electrochemical biosensors detect the electrical signal generated by biological reactions. In general, electrochemical biosensors work on the principle that many enzyme catalysis reactions consume or produce ions or electrons, causing some changes in the electrical properties of the solution that can be detected and used as a measurement parameter [66]. The high selectivity of electrochemical signals is one of their greatest advantages. Electrochemical biosensors can measure three types of electric signal such as current, potential difference and impedance, which are called amperometer, potentiometer, impedance biosensors. These types of biosensors have gained huge interest from researchers due to their sensitivity, portability, affordability and versatility [67]. Moreover, the surface of the electrode can be modified with nanomaterials such as carbon nanotubes (CNTs) and gold nanoparticles (AuNPs) to further increase their sensitivity and stability [68]. Additionally, electrochemical biosensors can be designed in various formats,

including disposable strips, microfluidic chips, and wearable devices, catering to different application needs [69].

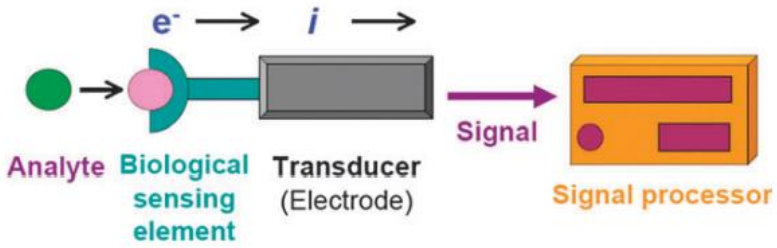

Figure 2.7 Schematic representation of components of an electrochemical biosensor [67]

Impedance Biosensors: Impedance-based electrochemical biosensors use the current response to a small AC voltage to detect changes in resistive and reactive properties at the electrode's surface. Impedance biosensors are ideal for point-of-care applications because they are inexpensive, easily miniaturized, and require simple instrumentation [70]. Numerous impedance-based biosensors have been developed for the detection of AFP biomarkers. Ciu et al designed an impedimetric biosensor by modifying glassy carbon electrode with poly3,4-ethyldioxythiophene [71]. Taheri et al imprinted plastic antibodies into the electropolymerized polypyrrole on a fluorine-doped tin oxide electrode for the detection of AFP and CEA [72].

Amperometric Biosensors: Amperometric biosensors monitor the current associated with oxidation or reduction of an electroactive species involved in the recognition process. An amperometric biosensor may be more attractive because of its high sensitivity and wide linear range [73]. Glucose biosensors are the most extensively researched amperometric biosensor, where glucose oxidase catalyzes the reaction between glucose and oxygen to produce gluconolactone and hydrogen peroxide [74]. Yuan et al designed an amperometric biosensor for AFP detection by immobilizing primary antibody on Fe_3O_4@Au nanoparticles with HRP and gold nanoparticle conjugated secondary antibody for signal amplification [75].

Potentiometric Biosensors: Potentiometric biosensors perform by tracking the change in potential at an ion-selective electrode (ISE) in response to the contact of the target analyte with a specific recognition element immobilized on the electrode surface [76]. Potentiometric sensors are small, have a rapid response, simple to use,

inexpensive, and resistant to color and turbid interferences [77] Qiang et al developed a potentiometric biosensor by immobilizing anti-AFP antibody on the surface of platinum disk electrode using gelatin-sliver film as a carrier [78].

Cyclic Voltammetry (CV): Cyclic voltammetry (CV) is a powerful and versatile electrochemical technique widely used to analyze the redox behavior of molecular species. The common applications of CV include the assessment of drug quality, determination of phenols and antioxidants, and detection of various biomolecules [79]. The applied voltage generates a potential for chemical reaction on the electrode surface, where the reactive molecule moves to the electrode surface for mass interaction, and the electrode receives the signal, resulting in a current flow across the electrode that can be measured cyclically. Conventional CV measurements are performed with a three-terminal configuration of cells that includes a working electrode, a counter electrode, and a reference electrode. The electrochemical reaction takes place in working electrode and ends the cycle at counter electrode, and reference is used as a reference point for other two electrodes [80].

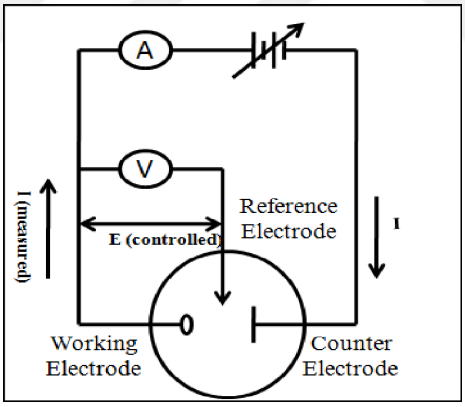

Figure 2.8 Simplified CV circuit diagram [81]

Figure 1.8 represents typical CV voltammogram where the sample starts its reduction and reaches its peak anodic current at E_{pa} until it reaches its switching potential. Following the switching potential, the sample starts its oxidation and reaches its cathodic peak current at E_{pc} until it reaches the starting point.

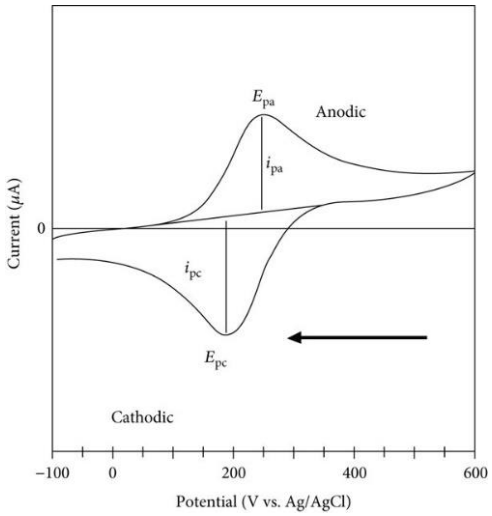

Figure 2.9 A CV voltammogram example [82]

3
MATERIALS AND METHODS

3.1 Materials

Chemicals: Distilled water, Rink Amide MBHA resin (with Norleucine), 11-Mercaptoundecaonic Acid. Acetic Anhydrous, Acetonitrile, Alpha fetoprotein (AFP), Bicinchoninic acid (BCA) Assay Kit, Biotin, Dimethyl Formamide (DMF), Dynabeads M-280 Streptavidin Magnetic Microbeads, Ethanol, Ethanolamine, Ferrocyanide, Fmoc-Alanine-OH, Fmoc-Histidine-OH Fmoc-Isoleucine-OH, Fmoc-Leucine-OH, Fmoc-Serine-OH, Fmoc-Threonine-OH, Fmoc-Tyrosine-OH, Fmoc-Valine-OH, Hexafluorophosphate Benzotriazole Tetramethyl Uronium (HBTU), N-Hydroxysuccinimide (NHS), N,N-Diisopropylethylamine (DIEA), N-(3-Dimethylaminopropyl)-N-Ethylcarbodiimide Hydrochloride (EDC), Phosphate Buffered Saline (PBS), Piperidine, Pyridine, Streptavidin, Trifluoracetic Acid (TFA), Triisopropylsilane (TIPS).

Instruments: Fume Hood was used for solid phase peptide synthesis. LC/MS Machine in Bilkent University National Nanotechnology Research Center (UNAM) was used for mass characterization of peptides. SHIMADZU Preparative Liquid Chromatography System with Thermo Scientific Hypersil GOLD C18 column (250 mm x 10.0 mm, 12 µm) was used for HPLC analysis. BioTek UV-Vis Plate Reader in Dr. Esin AKÇAEL's Genetic Engineering laboratory was used for UV measurements. EBTRO Potentiostat in Assoc. Dr. Prof. İlke GÜROL's Biophysics laboratory was used for CV measurements.

3.2 Peptide Synthesis

To select peptides with affinity for alpha fetoprotein (AFP) biomarkers, an extensive literature search was conducted and peptide sequences for AFP were identified from the literature. The peptides were taken from research on CDR region of human anti-AFP antibody, sequence of which was mapped by Hansen et al [83]. Identified peptide sequences were then undergone docking using the AutoDock CrankPep program, docking operations were docked here using the HPEPDOCK server by Dr. Sefer BADAY and his team with the help of Dr. Özgür YILMAZ and

his team. The sequences that had most affinity via docking have been selected as affinity molecules for AFP detection. Biotinylated SYVIH (Serine-Tyrosine-Valine-Isoleucine-Histidine) and YTSALLP (Tyrosine-Threonine-Serine-Alanine-Leucine-Leucine-Proline) peptides sequences have been selected and solid-phase peptide synthesis method been used to synthesize peptides. The synthesis was done in a fume hood with access to nitrogen gas. Before synthesis, 20% piperidine/DMF (v/v), Acetic anhydrous/pyridine/DMF (1:1:10) (v/v/v) solution was prepared.

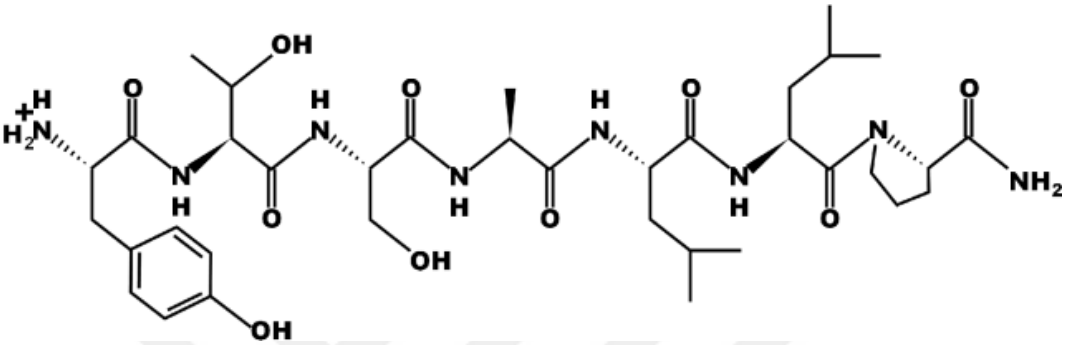

Figure 3.1 Structure of NH_2-YTSALLP-$CONH_2$ sequence

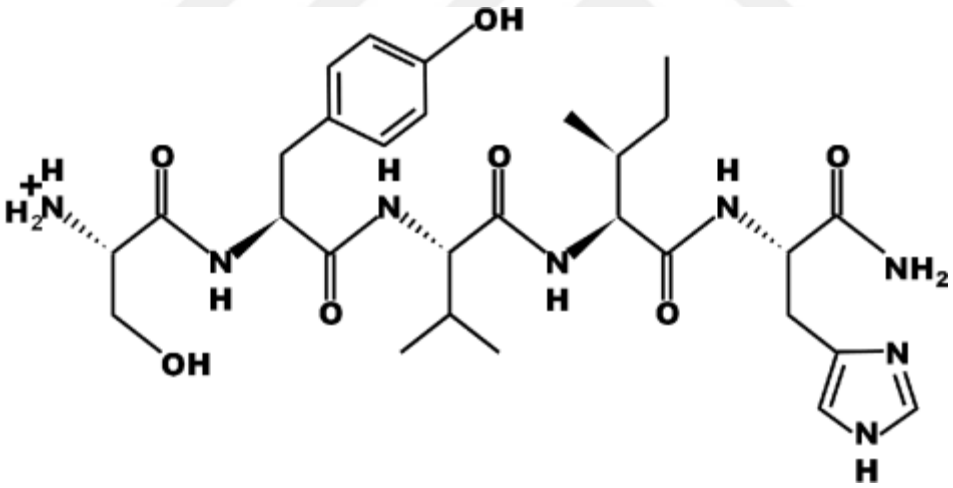

Figure 3.2 Structure of NH_2-SYVIH-$CONH_2$ sequence

The protocol of peptide synthesis is as follows:

1. 0.022 mmol rink amide MBHA resin (with Norleucine) was placed in the column and 5ml of DMF was added.
2. After an hour when the resin was swollen, DMF was removed from the column via vacuum.
3. The column was washed with 10 ml of DMF 3 times.
4. 1.5 ml of acetic anhydrous/pyridine/DMF (1:1:10)(v/v/v) solution was added into the column and waited for 10 minutes.

5. The solution was removed via vacuum and washed with 10 ml of DMF 2 times.
6. 2 ml of 20% piperidine/DMF (v/v) was added into the column and waited for 10 minutes and removed via vacuum twice.
7. The solution was removed via vacuum and washed with 10 ml DMF 3 times.
8. 0.121 mmol Fmoc-x-OH amino acid and 52 mg of HBTU was dissolved in 3ml of DMF and added into the column and stirred for 30 seconds.
9. 48 µl of DIEA was added into the column and stirred for 30 seconds and left for 1.5 hour minimum.
10. After the amino acids were added, steps 4-9 are repeated for each amino acid.
11. For biotin addition N-alpha-Fmoc-N-epsilon-(4-methyltrityl)-L-lysine was added and then 1% TFA solution in dichloromethane is used to break the methyltrityl protection group. After the color changed from white to yellow to white again the column was left overnight. 36,64 mg biotin, 80.8 mg HBTU, 85.2 µL DIEA in 6 ml of DMF was added and left overnight.
12. After adding biotin, the column was washed with 10 ml DMF and vacuum dried.
13. 4 ml of TFA/H_2O/TIPS (95:2.5:2.5)(v/v/v) was prepared. 2 ml of the solution was added into the column twice to terminate the peptide synthesis.

3.2.1 Peptide Characterization and Purification

Synthesized peptides were sent to Bilkent University National Nanotechnology Research Center (UNAM) for liquid chromatography/mass spectroscopy (LC/MS) to determine the molecular mass. If the obtained results correspond to theoretical value, then peptides are purified using gradient HPLC.

Peptides synthesized by solid state synthesis method are purified by RP-HPLC. It is performed on SHIMADZU Preparative Liquid Chromatography system with Thermo Scientific Hypersil GOLD C18 column (250 mm x 10.0 mm, 12 µm). In this step, peptides are prepared in high concentrations by dissolving in acetonitrile and distilled water. The syringe tip is passed through a filter (0.45 µm), transferred to a clean vial and injected into the device. Elution is performed using an acetonitrile/water gradient containing 0.08% trifluoroacetic acid. The acetonitrile concentration is increased from 1% to 100% over 55 min at a flow rate of 5 ml/min.

Column temperature is set to 40 °C and injection volume is set to 5000 µl. Detector response peaks are observed at a wavelength of 214 nm. During elution, when the detector peaks, peaks thought to be peptide peaks are collected in glass test tubes in the fraction collection area of the device. They are then transferred to clean glass containers and placed in a lyophilizer. After a 37-hour program, the solvents are completely evaporated and dried. The samples are then stored at -20 °C.

The purity of peptides is determined by analytical HPLC. For this procedure, an acetonitrile/water gradient containing 0.08% trifluoroacetic acid (TFA) is used as eluent. Acetonitrile is injected at a flow rate of 1 ml/min for 55 min, increasing the concentration from 1% to 100%. The injection volume is 25 µl and the column temperature is set to 40 °C. The purity of the peptides is calculated at 214 nm wavelength. The synthesis of peptides is evaluated by mass spectroscopy analysis.

3.3 Peptide Immobilization on Magnetic Beads

When the synthesized peptide achieves <%95 purity, then peptides are immobilized on commercially acquired Dynabeads M-280 Streptavidin. SYVIH and YTSALLP peptide showing AFP affinity was selected in the modelling for binding to Streptavidin coated MMBs. To determine the amount of peptide bound to MMBs, 100 µg of Streptavidin-coated MMBs and different concentrations of the peptide were used in a final volume of 100 µl. The presence of extra unbound peptides in the supernatant of the mixture, which reached saturation after binding to the available MMBs, was determined by BCA assay.

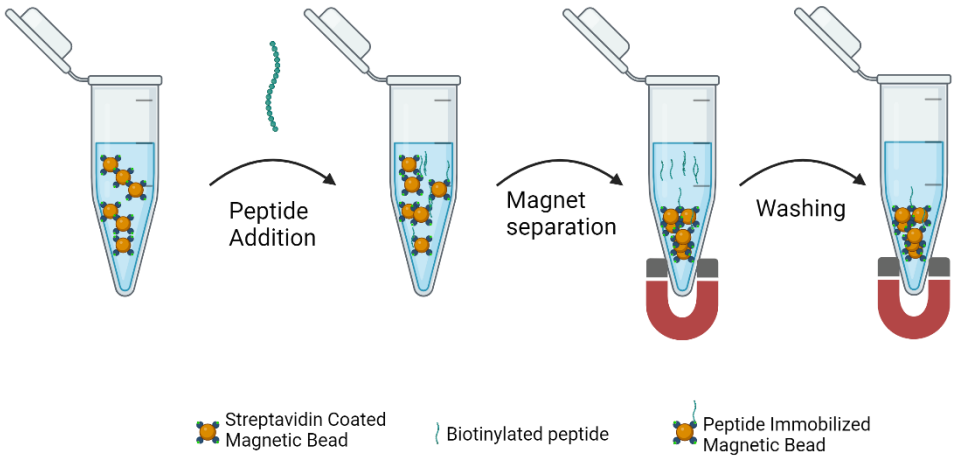

Figure 3.3 Schematic representation of peptide immobilization onto magnetic microbeads

Peptide conjugation to streptavidin-coated magnetic beads was performed as follows.

1. Magnetic beads were resuspended and 80 µl of 10 mg/ml MMB suspension was transferred to a vial and kept on the magnetic rack for 3 minutes. The supernatant was removed from the medium and MMBs were separated with the help of a magnet.
2. 80 µl of previously prepared PBS-T (0.1% Tween 20) buffer, pH 7.4 was added to the MMBs and vortexed for 10 seconds to suspend.
3. The resulting MMB suspension was transferred to different vials as 10 µl. Then different concentrations of peptide solutions were added to the vials with MMB suspension to a final volume of 100 µl and gently mixed for 30 minutes at room temperature. Then the suspension was kept in magnet for 3 minutes and the supernatant was transferred to a separate vial.
4. The supernatants were used to determine the amount of unbound peptide.
5. For calibration, different concentrations of peptides were mixed in PBS solution to a final volume of 100 µl.
6. The washing process was repeated 3 times with PBS. The supernatant was resuspended and kept on the magnet for 3 min and then the supernatant was separated for characterization.

3.3.1 BCA Assay

25 µl of peptide solution and supernatant of peptide-bead solution was added onto MicroWell™ 96-well plate. 200 µl of prepared BCA stock solution was added onto bead solutions, mixed and the samples were incubated at 37°C for 30 minutes and the absorbance of all samples was measured at 562 nm with BioTek UV-Vis Plate Reader.

A calibration curve was plotted from the absorbance of the peptide solution, establishing the relationship between peptide concentration and absorbance in the form of an equation. The obtained equation was then used to determine the concentration of the supernatant of peptide-bead solution and the amount of peptide

in the supernatant was then calculated. The peptide amount was then subtracted from the initial peptide amount and the amount of peptide bound to magnetic beads is obtained.

3.4 Peptide Immobilization on Gold Surface

Gold electrodes were manufactured, and plasma treated by Assoc. Prof. Ilke GÜROL's team. SYVIH peptide was selected to modify gold electrodes. Different concentrations of peptide (0.05,0.1,0.15.0.2 mg/ml) were added to coat gold electrodes. Before surface modification 10 mM 11-mercaptoundecaonic acid, 20 mM N-(3-dimethylaminopropyl)-N-ethylcarbodiimide hydrochloride (EDC) and 10 mM N-hydroxysuccinimide (NHS), and 10 mM ethanolamine solutions were prepared.

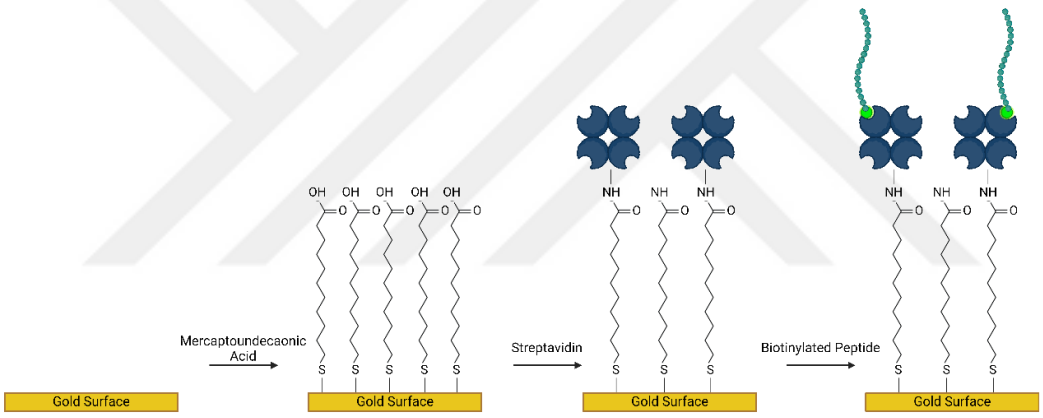

Figure 3.4 Schematic representation of peptide immobilization onto a gold surface

The modification of the gold surfaces was performed as follows:

1. Gold electrodes were washed with ethanol.
2. After washing the electrode surface, 25 µl of 10 mM 11-mercaptoundecaonic acid was added onto the gold surface.
3. After waiting overnight at 4℃, gold electrodes were washed with ethanol and dried via nitrogen.
4. The electric current of the acid modified electrode surfaces was measured.
5. 25 µl of 20 mM N-(3-dimethylaminopropyl)-N-ethylcarbodiimide hydrochloride (EDC) and 10 mM N-hydroxysuccinimide (NHS) solution was added onto the electrode surface.

6. After incubating for 1 hour at room temperature, gold electrodes were washed with PBS and dried via nitrogen.
7. 25 µl of Streptavidin (1 mg/ml) dissolved in water was added onto the electrode surface.
8. After incubating for one hour at room temperature, gold electrodes are washed with PBS and dried via nitrogen. and the electric current is measured.
9. The electric current of the streptavidin modified electrode surfaces are measured.
10. 25 µl of 10 mM ethanolamine is added onto the electrode surface.
11. After incubating for half an hour at room temperature, gold electrodes were washed with PBS and dried via nitrogen.
12. Biotinylated peptide was added onto the surface modified electrodes.
13. After waiting for half an hour at room temperature, gold electrodes were washed with PBS and dried via nitrogen.

3.4.1 CV Measurements

CV measurements of the modified electrodes were taken in Assoc. Prof. Dr. Ilke GÜROL's biophysics laboratory. The electric current of the surface modified electrodes was measured with an EBTRO Potentiostat device. 25 µl ferrocyanide solution was added on chips and their CV measurements were taken after each new molecule is immobilized. For final CV measurement of gold surface with AFP, 25 µl of 12000 pg/ml AFP solution was added onto a gold surface. The relationship of the voltage and the current was plotted, and the graph is smoothed using Origin Pro.

4
RESULTS AND DISCUSSION

4.1 Peptide Characterization

4.1.1 Results for YTSALLP peptide

The analytical HPLC result of the YTSALLP peptide chromatogram, and the peak value table of the chromatogram are shown. When the chromatogram and table are analyzed, it is observed that the purity peak of the peptide comes at 18.5 minutes. As a result of analytical HPLC, the purity value of the peak of the peptide was measured as 96.9%.

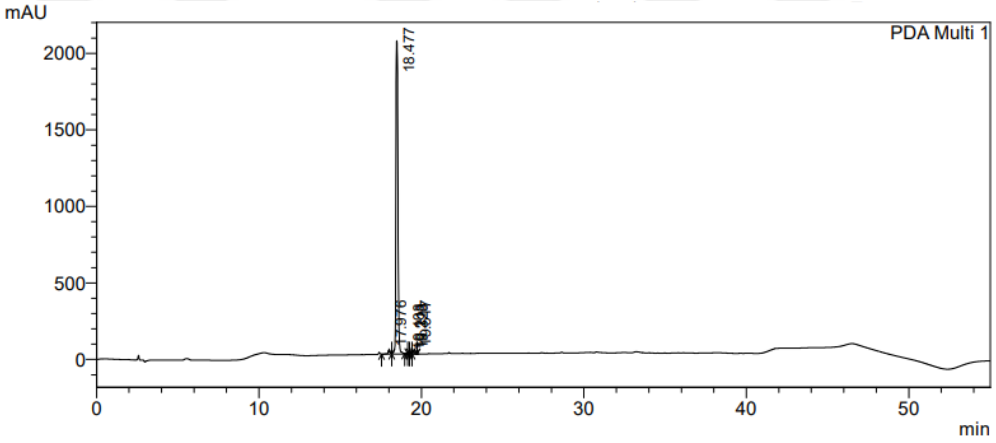

Figure 4.1 HPLC chromatogram of biotinylated YTSALLP peptide

Table 4.1 HPLC peak table of biotinylated YTSALLP peptide

PeakTable

PDA Ch1 214nm 4nm

Peak#	Ret. Time	Area	Height	Area %	Height %
1	17.976	242440	26550	1.303	1.257
2	18.477	18146315	2047267	97.535	96.942
3	19.103	22950	3147	0.123	0.149
4	19.218	22252	4089	0.120	0.194
5	19.323	32935	5658	0.177	0.268
6	19.517	138037	25141	0.742	1.190
Total		18604929	2111852	100.000	100.000

To confirm that the mass of synthesized peptide corresponds to its theoretical value, it was analyzed by mass spectrometry. The mass spectrum showed a mass-to-charge ratio of 1117.6. The theoretical value was calculated using “PepCalc.com peptide calculator” which calculated the theoretical mass of the peptide as 1117.36 g/mol.

It can be inferred that the synthesized peptide has correct sequence due to its experimental and mass value similarity [84], [85].

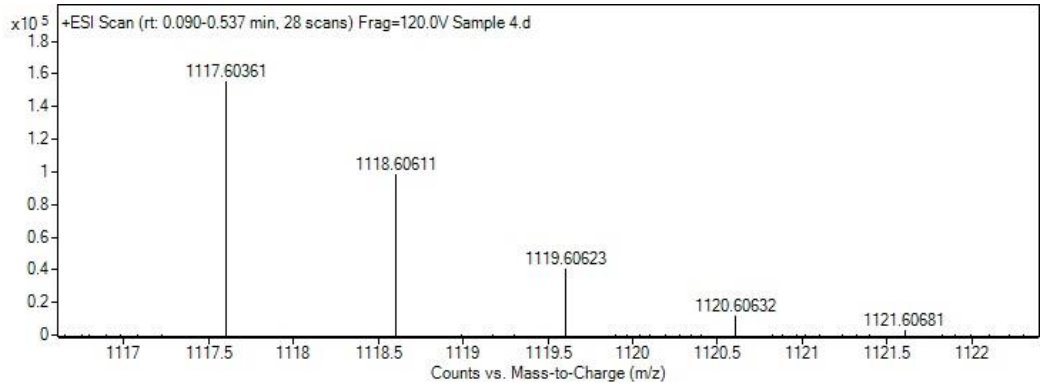

Figure 4.2 Mass spectrum of biotinylated YTSALLP peptide

4.1.2 Results for SYVIH peptide

The analytical HPLC result of the SYVIH peptide chromatogram, and the peak value table of the chromatogram are shown. When the chromatogram and table are analyzed, it is observed that the purity peak of the peptide comes at 16 minutes. As a result of analytical HPLC, the purity value of the peak of the peptide was measured as 95.4%.

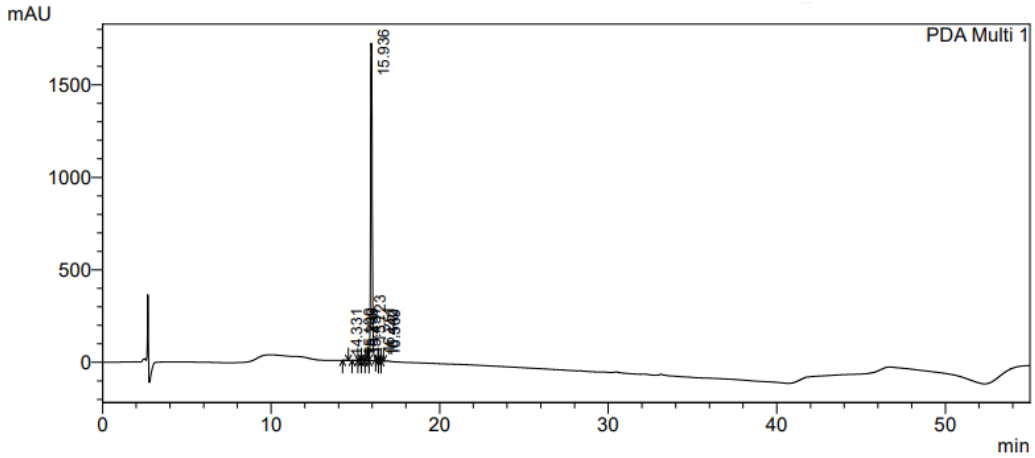

Figure 4.3 HPLC chromatogram biotinylated SYVIH peptide

Table 4.2 HPLC peak table of biotinylated SYVIH peptide

PeakTable

PDA Ch1 214nm 4nm

Peak#	Ret. Time	Area	Height	Area %	Height %
1	14.331	15250	2325	0.125	0.128
2	15.100	16071	1820	0.131	0.100
3	15.239	46232	6953	0.378	0.382
4	15.431	54007	7667	0.442	0.421
5	15.723	385417	73862	3.151	4.057
6	15.936	11664316	1715221	95.376	94.212
7	16.251	31820	8666	0.260	0.476
8	16.442	6543	1580	0.053	0.087
9	16.569	10194	2496	0.083	0.137
Total		12229849	1820590	100.000	100.000

To confirm that the mass of synthesized peptide corresponds to its theoretical value, it was analyzed by mass spectrometry. The mass spectrum showed a mass-to-charge ratio of 971.53. The theoretical value was calculated using "PepCalc.com peptide calculator" which calculated the theoretical mass of the peptide as 971.18 g/mol. It can be inferred that the synthesized peptide has correct sequence due to its experimental and mass value similarity [84], [85].

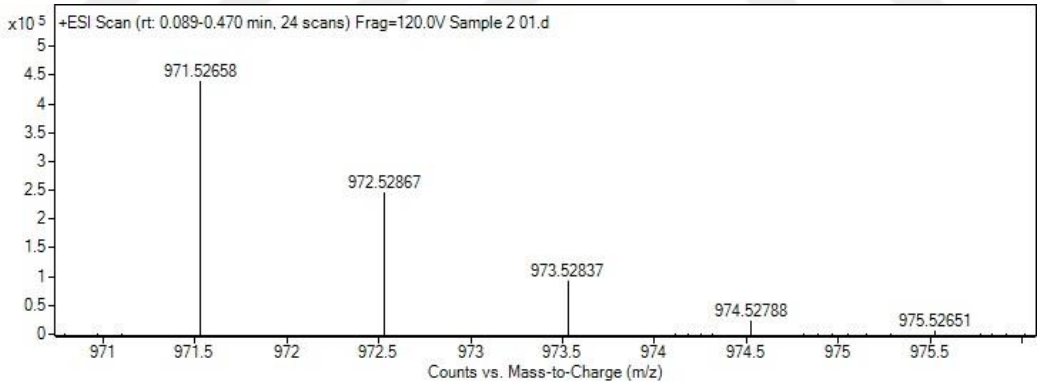

Figure 4.4 Mass spectrum of biotinylated SYVIH peptide

4.2 BCA Assay

Tripathi et al sought to create an antibody-bead system with high antibody coupling efficiency and minimize prep-to-prep variations to decrease the cost of the antibody-bead system for further biosensor applications by determining the amount of antibody required to saturate a fixed amount of beads [86]. To minimize the peptide consumption and create an optimal biosensor surface for AFP detection we sought to optimize the coupling efficiencies of peptide on our bead-peptide system.

To determine the binding efficiency of the peptides to beads a fixed amount of beads were coupled with different concentrations of peptides. Both peptides had similar graph to the one plotted by Tripathi et al and the optimal bead-peptide conditions were discovered.

4.2.1 Binding Capacity of YTSALLP

A calibration curve was created using peptide concentrations between 0-0.4 mg/ml. The equation obtained from the graph was used to calculate the bound peptide concentration on magnetic beads. The graph has an R value of 0.9895 which shows good linearity and can be used to calculate unknown samples.

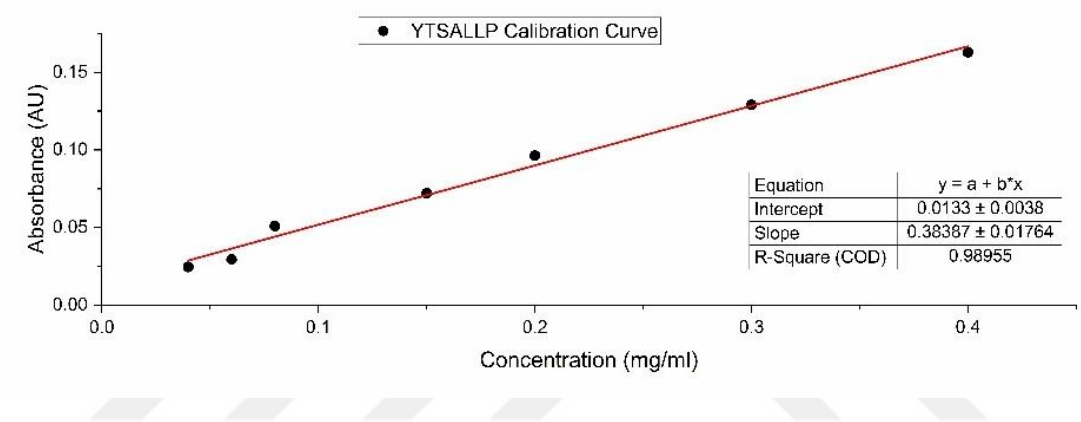

Figure 4.5 Calibration curve of YTSALLP peptide

The absorbance of supernatant of bead-peptide conjugation was measured to find the bound peptide concentration. The absorbance of supernatant was subtracted from initial concentration of peptide before magnetic bead conjugation to calculate the binding capacity. The graph was plotted for each initial concentration, and it was observed that peptide reaches its binding capacity at 59.8 ug/mg of bead at initial concentration of 0.25 mg/ml.

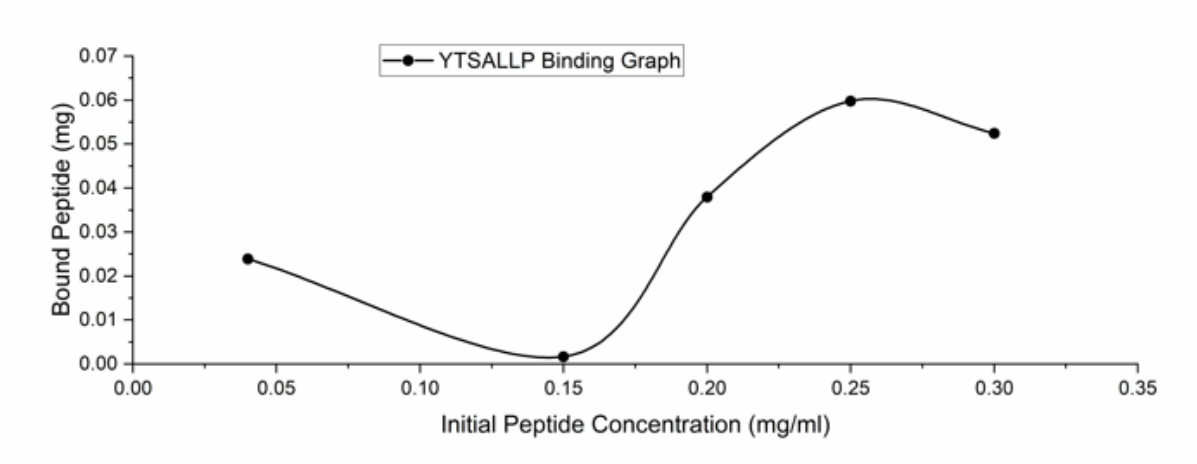

Figure 4.6 Binding graph of YTSALLP peptide

4.2.2 Binding Capacity of SYVIH

A calibration curve was created using peptide concentrations between 0-0.4 mg/ml. The equation obtained from the graph was used to calculate the bound peptide concentration on magnetic beads. The graph has an R value of 0.9837 which shows good linearity and can be used to calculate unknown samples.

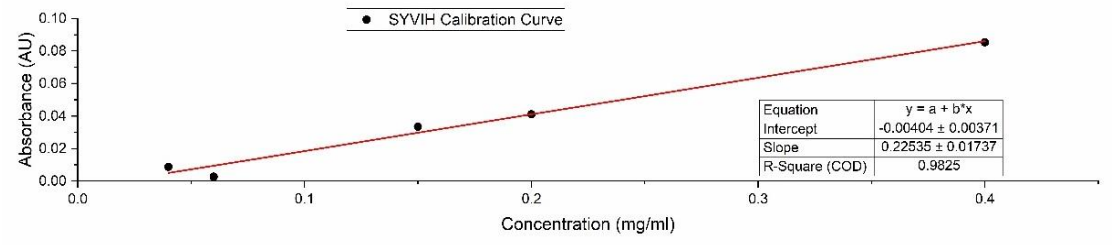

Figure 4.7 Calibration curve of SYVIH peptide

The absorbance of supernatant of bead-peptide conjugation was measured to find the bound peptide concentration. The absorbance of supernatant was subtracted from initial concentration of peptide before magnetic bead conjugation to calculate the binding capacity. The graph was plotted for each initial concentration, and it was observed that peptide reaches its binding capacity at 52 ug/mg of bead at initial concentration of 0.25 mg/ml.

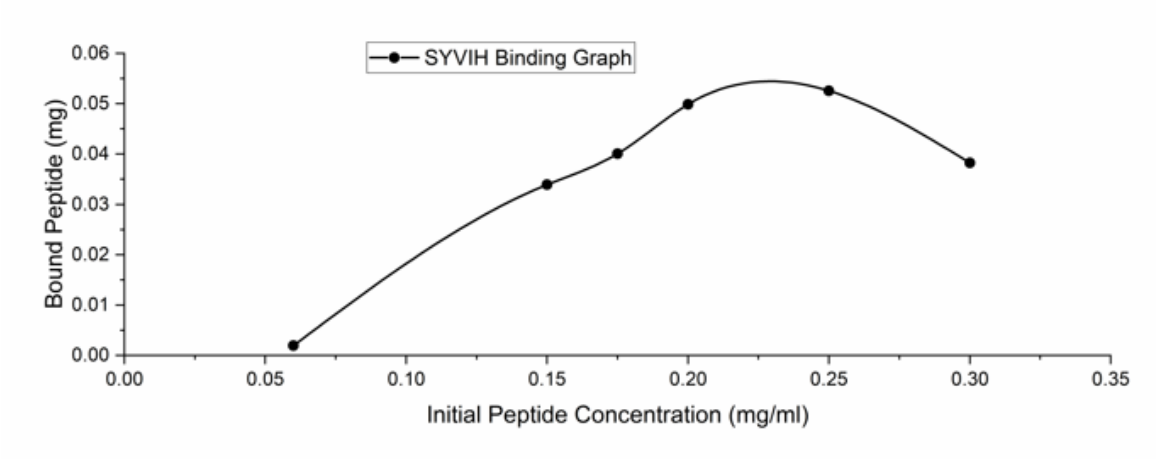

Figure 4.8 Binding graph of SYVIH peptide

4.3 CV Measurements

The CV measurements of SYVIH immobilized gold electrodes with peptide concentration 0.05, 0.1, 0.15, 0.2 mg/ml was taken. The maximum current for the gold electrodes was measured as 47.6, 46.1, 41.4 and 76.5 mA for concentrations of 0.05,0.1,0.15,0.2 mg/ml respectively. From the graphs it can be inferred that there is not a relationship that can be observed related to concentration with maximum current observed in 0.2 mg/ml peptide concentration. However, peptide immobilization with higher concentration showed better decrease in electrical current. This might happen dure to salts in PBS affecting the conductivity or MUA not fully coating the surface of the gold.

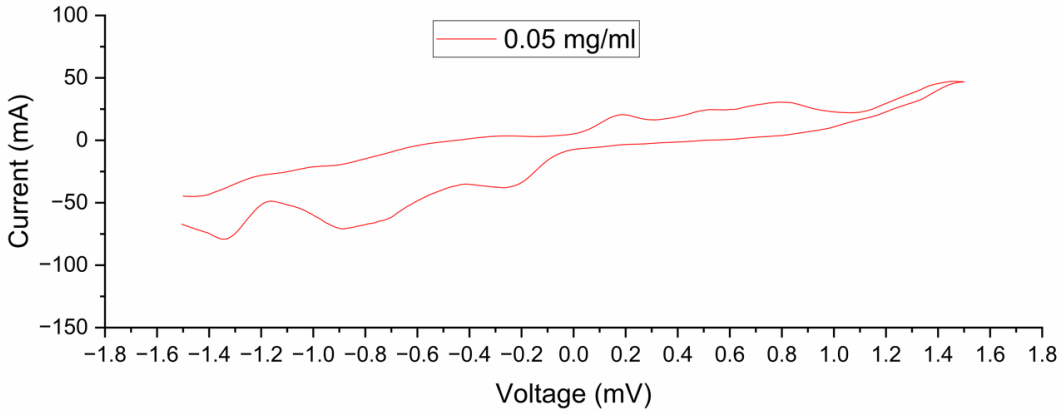

Figure 4.9 CV results of biotinylated SYVIH with a concentration of 0.05 mg/ml

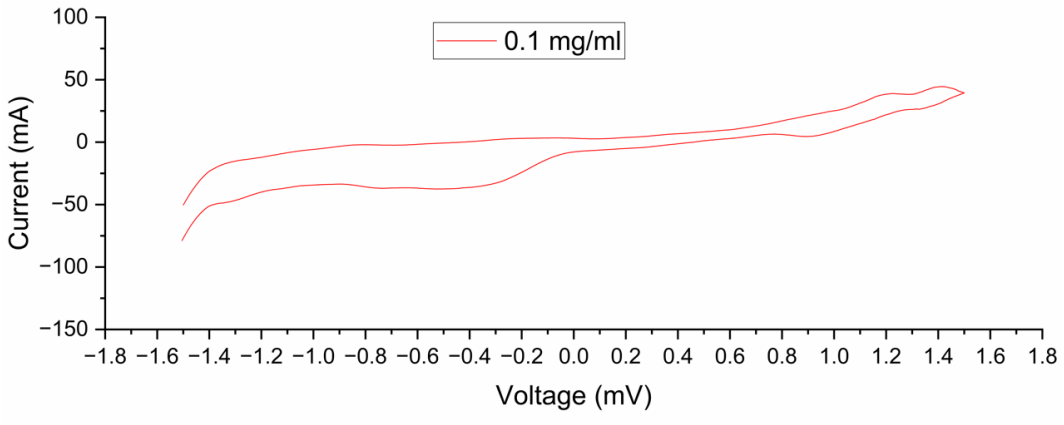

Figure 4.10 CV results of biotinylated SYVIH with a concentration of 0.1 mg/ml.

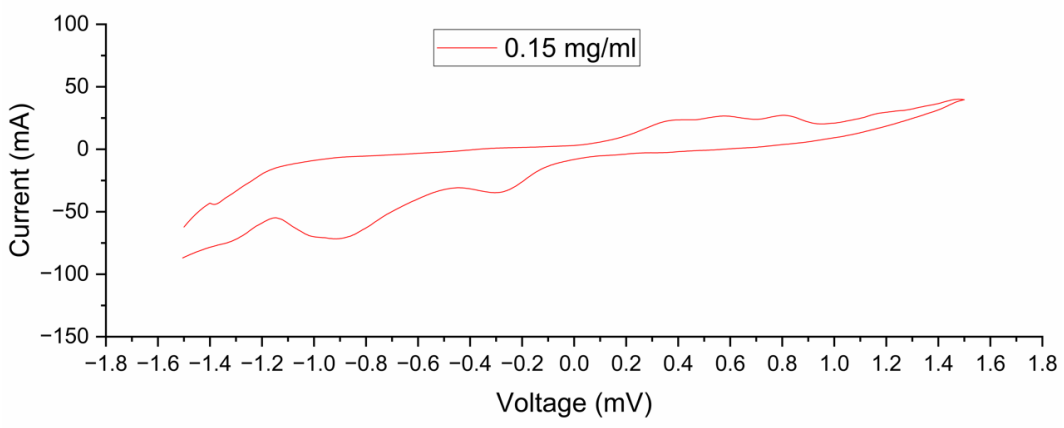

Figure 4.11 CV results of biotinylated SYVIH with a concentration of 0.15 mg/ml

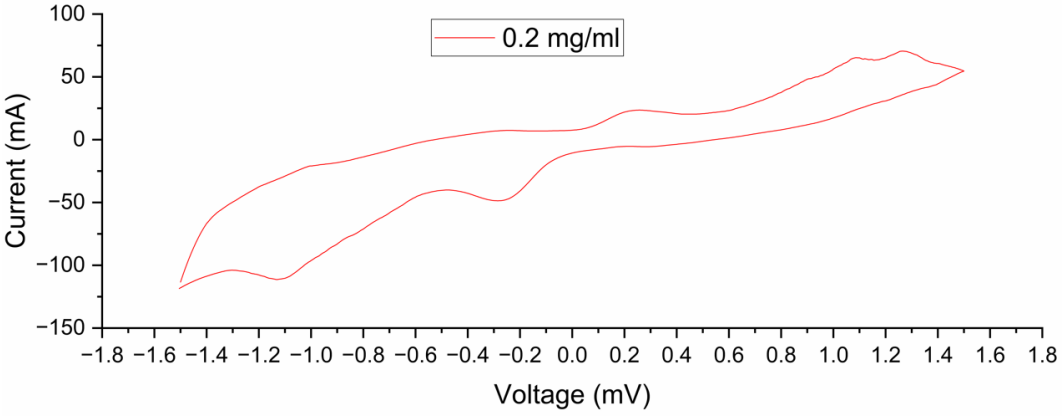

Figure 4.12 CV results of biotinylated SYVIH with a concentration of 0.2 mg/ml

CV measurements were also done to measure the relationship between SYVIH peptide and AFP protein. From the graph it can be inferred that the maximum current of a bare gold electrode is 20.5 mA and with the immobilization of chemicals the conductivity of the electrode decreases. The addition of MUA greatly inhibits the conductivity of gold electrode as the maximum current becomes 3.4 mA. The addition of SYVIH increases the maximum current to 4.4 and the final addition of AFP drops the maximum current to 3.04 mA. This result was somewhat similar to a result found by Zhao et al which showed a decreasing current signal with increasing AFP concentration. It can be inferred that there is a relationship between AFP and SYVIH. However, this relationship alone cannot guarantee SYVIH affinity and binding with AFP and further tests may be required.

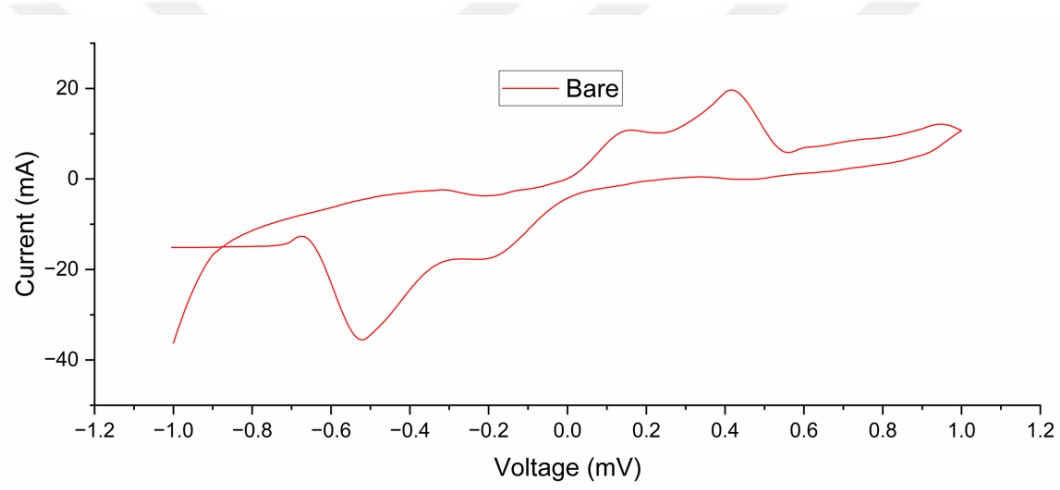

Figure 4.13 CV results of a bare gold electrode

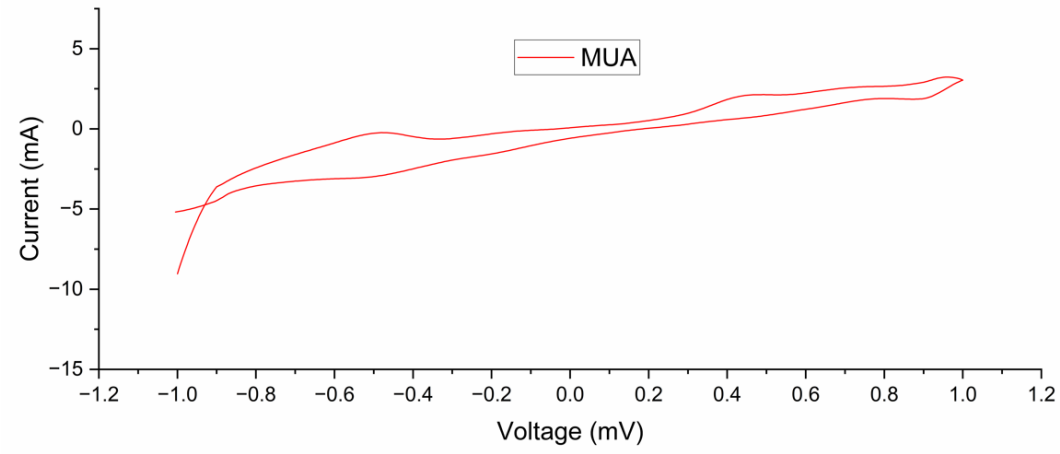

Figure 4.14 CV results of a gold electrode modified with MUA

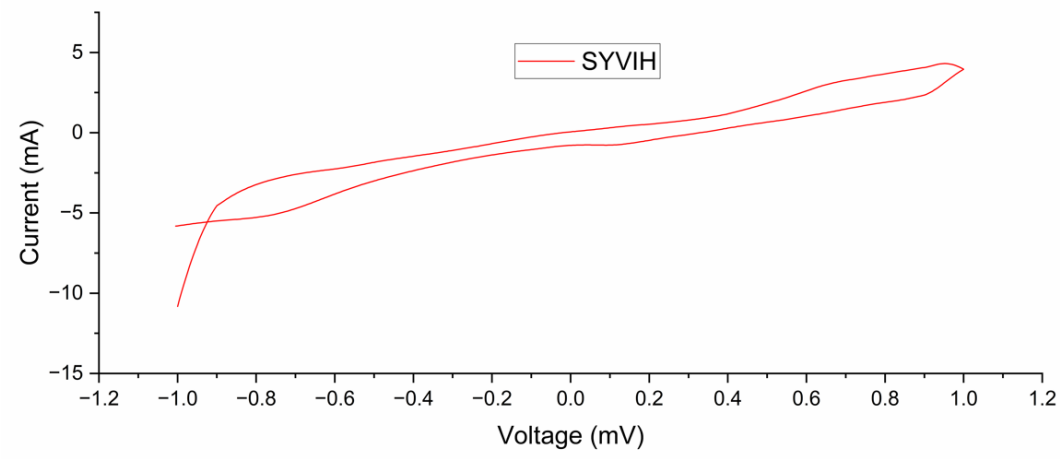

Figure 4.15 CV results of a gold electrode modified with SYVIH peptide

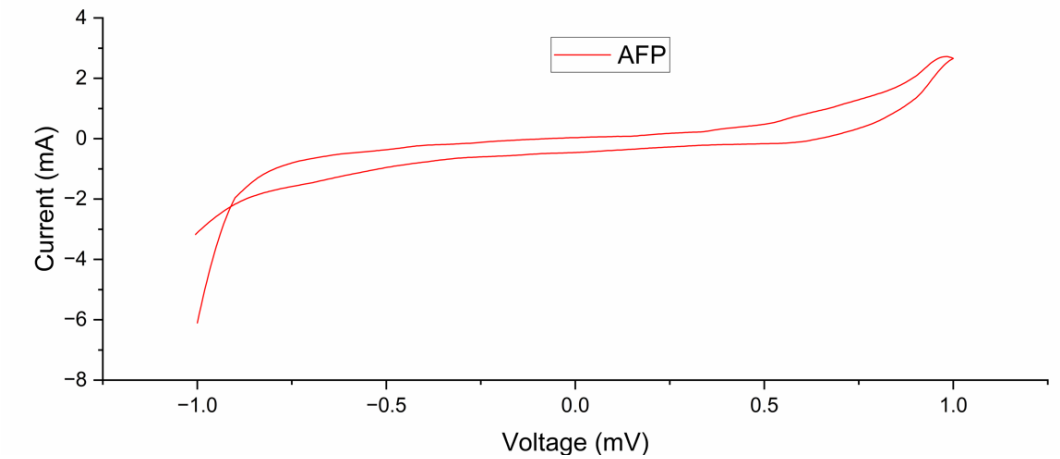

Figure 4.16 CV results of a gold electrode modified with AFP protein

5
CONCLUSION

The aim of this thesis is to aid in the development of a potential surface for detection of hepatocellular carcinoma. Peptide sequences determined from Complementarity Determining Region (CDR) of human anti-AFP antibody were chosen for AFP detection. In this thesis, the peptides were synthesized using solid-phase peptide synthesis method and immobilized into magnetic beads and gold electrodes. After immobilization of the peptides, the relationship of the surface with the peptides was measured.

AFP has low sensitivity towards HCC, especially in the early stages. Studies have shown that AFP gives reliable results largely in later stages when the tumor burden is higher. Aptamers have an advantage over due to their simplicity, stability, and affordability. Relying on these advantages, aptamers can be a great tool for increasing the sensitivity of AFP biosensors, thus reducing the time when sensor can detect HCC, thus making it easier to treat.

The peptides were synthesized using solid-phase peptide synthesis on a glass column on rink amide MBHA resin (with Norleucine). After the synthesis, peptides were modified with biotin because of its selective binding to streptavidin. Modified peptides were then immobilized onto magnetic microbeads and gold electrodes to observe their interactions with various surfaces.

The concentration of immobilized peptides streptavidin coated magnetic microbeads were determined using bicinchoninic acid assay (BCA) and the optimum concentration of peptide per mg of bead was determined. Both YTSALLP and SYVIH peptides showed optimum binding at the initial concentration of 0.25 mg/ml peptide per 0.1 mg of beads with binding of 59.8 mg/mg and 52 mg/mg respectively. Both peptides showed somewhat similar optimum concentration when conjugated with streptavidin coated magnetic beads. Peptide conjugated beads can be used in a variety of HCC related biosensor applications such as microchannel binding and magnetic enzyme-linked immunosorbent assay (MELISA) due to their easiness of immobilization and release using magnets.

SYVIH peptide also was immobilized onto gold surfaces and its cyclic voltammetry measurements were taken to determine its relationship with gold surface and AFP. CV measurements of peptide in different concentration showed somewhat irregular results which might be the result of PBS influence on conductivity or MUA not fully coating the surface. However, SYVIH immobilization on higher concentrations showed a greater reduction in conductivity. After immobilization the peptide inhibited the conductivity of the gold surface and addition of AFP further inhibited the conductivity. However, the addition of peptides onto gold surfaces in different concentrations showed somewhat different results with the highest concentration having highest conductivity. From the CV measurements it can be inferred that addition of AFP changed the conductivity of the gold electrode and it can show that SYVIH and AFP interacted. However, this cannot be used as proof that AFP selectively binds to SYVIH peptide and further analyses are needed.

REFERENCES

[1] Ferlay J *et al.*, "Global Cancer Observatory: Cancer Today. Lyon, France: International Agency for Research on Cancer." Accessed: Jul. 13, 2024. [Online]. Available: https://gco.iarc.who.int/today

[2] F. P. Russo *et al.*, "Hepatocellular Carcinoma in Chronic Viral Hepatitis: Where Do We Stand?," *Int J Mol Sci*, vol. 23, no. 1, p. 500, Jan. 2022, doi: 10.3390/ijms23010500.

[3] J. M. Llovet *et al.*, "Hepatocellular carcinoma," *Nat Rev Dis Primers*, vol. 10, no. 1, p. 10, Feb. 2024, doi: 10.1038/s41572-024-00500-6.

[4] N. D. Parikh, A. S. Mehta, A. G. Singal, T. Block, J. A. Marrero, and A. S. Lok, "Biomarkers for the Early Detection of Hepatocellular Carcinoma," *Cancer Epidemiology, Biomarkers & Prevention*, vol. 29, no. 12, pp. 2495–2503, Dec. 2020, doi: 10.1158/1055-9965.EPI-20-0005.

[5] X. Wei *et al.*, "Quantitative proteomic profiling of hepatocellular carcinoma at different serum alpha-fetoprotein level," *Transl Oncol*, vol. 20, p. 101422, Jun. 2022, doi: 10.1016/j.tranon.2022.101422.

[6] B. Lin *et al.*, "Structural basis for alpha fetoprotein-mediated inhibition of caspase-3 activity in hepatocellular carcinoma cells," *Int J Cancer*, vol. 141, no. 7, pp. 1413–1421, Oct. 2017, doi: 10.1002/ijc.30850.

[7] Y. Lu *et al.*, "Alpha fetoprotein plays a critical role in promoting metastasis of hepatocellular carcinoma cells," *J Cell Mol Med*, vol. 20, no. 3, pp. 549–558, Mar. 2016, doi: 10.1111/jcmm.12745.

[8] H. Hanif *et al.*, "Update on the applications and limitations of alpha-fetoprotein for hepatocellular carcinoma," *World J Gastroenterol*, vol. 28, no. 2, pp. 216–229, Jan. 2022, doi: 10.3748/wjg.v28.i2.216.

[9] P. Luo *et al.*, "Current Status and Perspective Biomarkers in AFP Negative HCC: Towards Screening for and Diagnosing Hepatocellular Carcinoma at an Earlier Stage," *Pathology & Oncology Research*, vol. 26, no. 2, pp. 599–603, Apr. 2020, doi: 10.1007/s12253-019-00585-5.

[10] C. BAYRAÇ, A. T. BAYRAÇ, E. SARIKAYA, and M. VARÇİN, "Adsorption of DNA on Coated Magnetic Beads: Comparison of Physical and Chemical Adsorption," *Erzincan Üniversitesi Fen Bilimleri Enstitüsü Dergisi*, vol. 12, no. 1, pp. 215–224, Mar. 2019, doi: 10.18185/erzifbed.442557.

[11] N. Kovačević, "Magnetic Beads Based Nucleic Acid Purification for Molecular Biology Applications," 2016, pp. 53–67. doi: 10.1007/978-1-4939-3185-9_5.

[12] N. Bhalla, P. Jolly, N. Formisano, and P. Estrela, "Introduction to biosensors," *Essays Biochem*, vol. 60, no. 1, pp. 1–8, Jun. 2016, doi: 10.1042/EBC20150001.

[13] S. Vigneshvar, C. C. Sudhakumari, B. Senthilkumaran, and H. Prakash, "Recent Advances in Biosensor Technology for Potential Applications – An Overview," *Front Bioeng Biotechnol*, vol. 4, Feb. 2016, doi: 10.3389/fbioe.2016.00011.

[14] N. Sewald and H. Jakubke, *Peptides: Chemistry and Biology*. Wiley, 2009. doi: 10.1002/9783527626038.

[15] S. Naisam, V. Selvaraj, and N. Sreekumar, "Peptides: antimicrobial properties and applications," *International Journal of Environmental Technology and Management*, vol. 25, no. 3, p. 233, 2022, doi: 10.1504/IJETM.2022.122648.

[16] S. Ståhl, T. Gräslund, A. Eriksson Karlström, F. Y. Frejd, P.-Å. Nygren, and J. Löfblom, "Affibody Molecules in Biotechnological and Medical Applications," *Trends Biotechnol*, vol. 35, no. 8, pp. 691–712, Aug. 2017, doi: 10.1016/j.tibtech.2017.04.007.

[17] J. Löfblom, J. Feldwisch, V. Tolmachev, J. Carlsson, S. Ståhl, and F. Y. Frejd, "Affibody molecules: Engineered proteins for therapeutic, diagnostic and biotechnological applications," *FEBS Lett*, vol. 584, no. 12, pp. 2670–2680, Jun. 2010, doi: 10.1016/j.febslet.2010.04.014.

[18] D. Dimitroulis *et al.*, "From diagnosis to treatment of hepatocellular carcinoma: An epidemic problem for both developed and developing world,"

World J Gastroenterol, vol. 23, no. 29, p. 5282, 2017, doi: 10.3748/wjg.v23.i29.5282.

[19] B. Alawyia and C. Constantinou, "Hepatocellular Carcinoma: a Narrative Review on Current Knowledge and Future Prospects," *Curr Treat Options Oncol*, vol. 24, no. 7, pp. 711–724, Jul. 2023, doi: 10.1007/s11864-023-01098-9.

[20] W. Abdelhamed and M. El-Kassas, "Hepatocellular carcinoma recurrence: Predictors and management," *Liver Res*, vol. 7, no. 4, pp. 321–332, Dec. 2023, doi: 10.1016/j.livres.2023.11.004.

[21] K. A. McGlynn, J. L. Petrick, and H. B. El-Serag, "Epidemiology of Hepatocellular Carcinoma," *Hepatology*, vol. 73, no. S1, pp. 4–13, Jan. 2021, doi: 10.1002/hep.31288.

[22] J. Balogh *et al.*, "Hepatocellular carcinoma: a review," *J Hepatocell Carcinoma*, vol. Volume 3, pp. 41–53, Oct. 2016, doi: 10.2147/JHC.S61146.

[23] D. L. White, S. Tavakoli-Tabasi, J. Kuzniarek, R. Pascua, D. J. Ramsey, and H. B. El-Serag, "Higher serum testosterone is associated with increased risk of advanced hepatitis C-related liver disease in males," *Hepatology*, vol. 55, no. 3, pp. 759–768, Mar. 2012, doi: 10.1002/hep.24618.

[24] J.-Y. Choi, J.-M. Lee, and C. B. Sirlin, "CT and MR Imaging Diagnosis and Staging of Hepatocellular Carcinoma: Part II. Extracellular Agents, Hepatobiliary Agents, and Ancillary Imaging Features," *Radiology*, vol. 273, no. 1, pp. 30–50, Oct. 2014, doi: 10.1148/radiol.14132362.

[25] R. Masuzaki and M. Omata, "Screening Program in High-Risk Populations," in *Hepatocellular Carcinoma:*, New York, NY: Springer New York, 2011, pp. 55–68. doi: 10.1007/978-1-60327-522-4_4.

[26] "Pathophysiology of HCC", doi: 10.1007/978-3-319-09414-4__4.

[27] S. Tanwar, F. Rhodes, A. Srivastava, P. M. Trembling, and W. M. Rosenberg, "Inflammation and fibrosis in chronic liver diseases including non-alcoholic fatty liver disease and hepatitis C," *World J Gastroenterol*, vol. 26, no. 2, pp. 109–133, Jan. 2020, doi: 10.3748/wjg.v26.i2.109.

[28] X. W. Wang *et al.*, "Molecular pathogenesis of human hepatocellular carcinoma," *Toxicology*, vol. 181–182, pp. 43–47, Dec. 2002, doi: 10.1016/S0300-483X(02)00253-6.

[29] R. N. Aravalli and C. J. Steer, "Pathophysiology of HCC," in *Hepatocellular Carcinoma*, Cham: Springer International Publishing, 2014, pp. 15–32. doi: 10.1007/978-3-319-09414-4_4.

[30] A. Maia and S. Wiemann, "Cancer-Associated Fibroblasts: Implications for Cancer Therapy," *Cancers (Basel)*, vol. 13, no. 14, p. 3526, Jul. 2021, doi: 10.3390/cancers13143526.

[31] H. Chen, J. Chen, H. Yuan, X. Li, and W. Li, "Hypoxia-inducible factor-1α: A critical target for inhibiting the metastasis of hepatocellular carcinoma (Review)," *Oncol Lett*, vol. 24, no. 2, p. 284, Jun. 2022, doi: 10.3892/ol.2022.13404.

[32] A. Jaffe, T. H. Taddei, E. G. Giannini, Y. C. Ilagan-Ying, M. Colombo, and M. Strazzabosco, "Holistic management of hepatocellular carcinoma: The hepatologist's comprehensive playbook," *Liver International*, vol. 42, no. 12, pp. 2607–2619, Dec. 2022, doi: 10.1111/liv.15432.

[33] W. Jarnagin *et al.*, "Surgical treatment of hepatocellular carcinoma: expert consensus statement," *HPB*, vol. 12, no. 5, pp. 302–310, Jun. 2010, doi: 10.1111/j.1477-2574.2010.00182.x.

[34] Y. Yamashita *et al.*, "Trends in surgical results of hepatic resection for hepatocellular carcinoma: 1,000 consecutive cases over 20 years in a single institution," *The American Journal of Surgery*, vol. 207, no. 6, pp. 890–896, Jun. 2014, doi: 10.1016/j.amjsurg.2013.07.028.

[35] K. W. Ma and T. T. Cheung, "When to Consider Liver Transplantation in Hepatocellular Carcinoma Patients?," *Hepat Oncol*, vol. 4, no. 1, pp. 15–24, Jan. 2017, doi: 10.2217/hep-2016-0010.

[36] E. Kotsifa *et al.*, "Transarterial Chemoembolization for Hepatocellular Carcinoma: Why, When, How?," *J Pers Med*, vol. 12, no. 3, p. 436, Mar. 2022, doi: 10.3390/jpm12030436.

[37] W. Badar, Q. Yu, M. Patel, and O. Ahmed, “Transarterial Radioembolization for Management of Hepatocellular Carcinoma,” *Oncologist*, Dec. 2023, doi: 10.1093/oncolo/oyad327.

[38] C. De Mees, J. Bakker, J. Szpirer, and C. Szpirer, “Alpha-Fetoprotein: From a Diagnostic Biomarker to a Key Role in Female Fertility.”

[39] X. Hu, R. Chen, Q. Wei, and X. Xu, “The Landscape Of Alpha Fetoprotein In Hepatocellular Carcinoma: Where Are We?,” *Int J Biol Sci*, vol. 18, no. 2, pp. 536–551, 2022, doi: 10.7150/ijbs.64537.

[40] K. Liu *et al.*, “Structural characteristics of alpha-fetoprotein, including N-glycosylation, metal ion and fatty acid binding sites,” *Commun Biol*, vol. 7, no. 1, p. 505, Apr. 2024, doi: 10.1038/s42003-024-06219-0.

[41] Y. Zheng, M. Zhu, and M. Li, “Effects of alpha-fetoprotein on the occurrence and progression of hepatocellular carcinoma,” *J Cancer Res Clin Oncol*, vol. 146, no. 10, pp. 2439–2446, Oct. 2020, doi: 10.1007/s00432-020-03331-6.

[42] S. Jin *et al.*, “Emerging new therapeutic antibody derivatives for cancer treatment,” *Signal Transduct Target Ther*, vol. 7, no. 1, p. 39, Feb. 2022, doi: 10.1038/s41392-021-00868-x.

[43] A. M. Scott, J. D. Wolchok, and L. J. Old, “Antibody therapy of cancer,” *Nat Rev Cancer*, vol. 12, no. 4, pp. 278–287, Apr. 2012, doi: 10.1038/nrc3236.

[44] A. Roy, S. Nair, N. Sen, N. Soni, and M. S. Madhusudhan, “In silico methods for design of biological therapeutics,” *Methods*, vol. 131, pp. 33–65, Dec. 2017, doi: 10.1016/j.ymeth.2017.09.008.

[45] J. Byun, “Recent Progress and Opportunities for Nucleic Acid Aptamers,” *Life*, vol. 11, no. 3, p. 193, Feb. 2021, doi: 10.3390/life11030193.

[46] J. Byun, “Recent Progress and Opportunities for Nucleic Acid Aptamers,” *Life*, vol. 11, no. 3, p. 193, Feb. 2021, doi: 10.3390/life11030193.

[47] V. Tolmachev and A. Orlova, “Affibody Molecules as Targeting Vectors for PET Imaging,” *Cancers (Basel)*, vol. 12, no. 3, p. 651, Mar. 2020, doi: 10.3390/cancers12030651.

[48] R. B. Merrifield, “Solid Phase Peptide Synthesis. I. The Synthesis of a Tetrapeptide,” *J Am Chem Soc*, vol. 85, no. 14, pp. 2149–2154, Jul. 1963, doi: 10.1021/ja00897a025.

[49] H. Masui and S. Fuse, “Recent Advances in the Solid- and Solution-Phase Synthesis of Peptides and Proteins Using Microflow Technology,” *Org Process Res Dev*, vol. 26, no. 6, pp. 1751–1765, Jun. 2022, doi: 10.1021/acs.oprd.2c00074.

[50] L. Wang *et al.*, “Therapeutic peptides: current applications and future directions,” *Signal Transduct Target Ther*, vol. 7, no. 1, p. 48, Feb. 2022, doi: 10.1038/s41392-022-00904-4.

[51] M. Amblard, J.-A. Fehrentz, J. Martinez, and G. Subra, “Methods and Protocols of Modern Solid Phase Peptide Synthesis,” *Mol Biotechnol*, vol. 33, no. 3, pp. 239–254, 2006, doi: 10.1385/MB:33:3:239.

[52] R. Behrendt, P. White, and J. Offer, “Advances in Fmoc solid-phase peptide synthesis,” *Journal of Peptide Science*, vol. 22, no. 1, pp. 4–27, Jan. 2016, doi: 10.1002/psc.2836.

[53] S. Berensmeier, “Magnetic particles for the separation and purification of nucleic acids,” *Appl Microbiol Biotechnol*, vol. 73, no. 3, pp. 495–504, Dec. 2006, doi: 10.1007/s00253-006-0675-0.

[54] H. Modh, T. Scheper, and J.-G. Walter, “Aptamer-Modified Magnetic Beads in Biosensing,” *Sensors*, vol. 18, no. 4, p. 1041, Mar. 2018, doi: 10.3390/s18041041.

[55] L. F. Huergo *et al.*, “Magnetic Bead-Based Immunoassay Allows Rapid, Inexpensive, and Quantitative Detection of Human SARS-CoV-2 Antibodies,” *ACS Sens*, vol. 6, no. 3, pp. 703–708, Mar. 2021, doi: 10.1021/acssensors.0c02544.

[56] C. Chen and J. Wang, “Optical biosensors: an exhaustive and comprehensive review,” *Analyst*, vol. 145, no. 5, pp. 1605–1628, 2020, doi: 10.1039/C9AN01998G.

[57] P. Damborský, J. Švitel, and J. Katrlík, “Optical biosensors,” *Essays Biochem*, vol. 60, no. 1, pp. 91–100, Jun. 2016, doi: 10.1042/EBC20150010.

[58] A. T. Kal-Koshvandi, “Recent advances in optical biosensors for the detection of cancer biomarker α-fetoprotein (AFP),” *TrAC Trends in Analytical Chemistry*, vol. 128, p. 115920, Jul. 2020, doi: 10.1016/j.trac.2020.115920.

[59] C. M. Miyazaki, F. M. Shimizu, and M. Ferreira, “Surface Plasmon Resonance (SPR) for Sensors and Biosensors,” in *Nanocharacterization Techniques*, Elsevier, 2017, pp. 183–200. doi: 10.1016/B978-0-323-49778-7.00006-0.

[60] S. Das, R. Devireddy, and M. R. Gartia, “Surface Plasmon Resonance (SPR) Sensor for Cancer Biomarker Detection,” *Biosensors (Basel)*, vol. 13, no. 3, p. 396, Mar. 2023, doi: 10.3390/bios13030396.

[61] H. Wang, X. Wang, J. Wang, W. Fu, and C. Yao, “A SPR biosensor based on signal amplification using antibody-QD conjugates for quantitative determination of multiple tumor markers,” *Sci Rep*, vol. 6, no. 1, p. 33140, Sep. 2016, doi: 10.1038/srep33140.

[62] X. Huang and J. Ren, “Gold nanoparticles based chemiluminescent resonance energy transfer for immunoassay of alpha fetoprotein cancer marker,” *Anal Chim Acta*, vol. 686, no. 1–2, pp. 115–120, Feb. 2011, doi: 10.1016/j.aca.2010.11.043.

[63] P. Audebert and F. Miomandre, “Electrofluorochromism: from molecular systems to set-up and display,” *Chem. Sci.*, vol. 4, no. 2, pp. 575–584, 2013, doi: 10.1039/C2SC21503A.

[64] S. Xu *et al.*, “Aptamer induced multicoloured Au NCs-MoS2 ‘switch on’ fluorescence resonance energy transfer biosensor for dual color simultaneous detection of multiple tumor markers by single wavelength excitation,” *Anal Chim Acta*, vol. 983, pp. 173–180, Aug. 2017, doi: 10.1016/j.aca.2017.06.023.

[65] L. Guo *et al.*, “Enhanced fluorescence detection of proteins using ZnO nanowires integrated inside microfluidic chips,” *Biosens Bioelectron*, vol. 99, pp. 368–374, Jan. 2018, doi: 10.1016/j.bios.2017.08.003.

[66] A. Singh *et al.*, “Recent Advances in Electrochemical Biosensors: Applications, Challenges, and Future Scope,” *Biosensors (Basel)*, vol. 11, no. 9, p. 336, Sep. 2021, doi: 10.3390/bios11090336.

[67] N. J. Ronkainen, H. B. Halsall, and W. R. Heineman, “Electrochemical biosensors,” *Chem Soc Rev*, vol. 39, no. 5, p. 1747, 2010, doi: 10.1039/b714449k.

[68] A. Curulli, “Nanomaterials in Electrochemical Sensing Area: Applications and Challenges in Food Analysis,” *Molecules*, vol. 25, no. 23, p. 5759, Dec. 2020, doi: 10.3390/molecules25235759.

[69] P. C. Ferreira *et al.*, “Wearable electrochemical sensors for forensic and clinical applications,” *TrAC Trends in Analytical Chemistry*, vol. 119, p. 115622, Oct. 2019, doi: 10.1016/j.trac.2019.115622.

[70] A. Chakraborty, D. N. Tibarewala, and A. Barui, “Impedance-based biosensors,” in *Bioelectronics and Medical Devices*, Elsevier, 2019, pp. 97–122. doi: 10.1016/B978-0-08-102420-1.00005-4.

[71] M. Cui, Z. Song, Y. Wu, B. Guo, X. Fan, and X. Luo, “A highly sensitive biosensor for tumor maker alpha fetoprotein based on poly(ethylene glycol) doped conducting polymer PEDOT,” *Biosens Bioelectron*, vol. 79, pp. 736–741, May 2016, doi: 10.1016/j.bios.2016.01.012.

[72] N. Taheri, H. Khoshsafar, M. Ghanei, A. Ghazvini, and H. Bagheri, “Dual-template rectangular nanotube molecularly imprinted polypyrrole for label-free impedimetric sensing of AFP and CEA as lung cancer biomarkers,” *Talanta*, vol. 239, p. 123146, Mar. 2022, doi: 10.1016/j.talanta.2021.123146.

[73] J. Wang, “Amperometric biosensors for clinical and therapeutic drug monitoring: a review,” *J Pharm Biomed Anal*, vol. 19, no. 1–2, pp. 47–53, Feb. 1999, doi: 10.1016/S0731-7085(98)00056-9.

[74] B. Lakard, “Electrochemical Biosensors Based on Conducting Polymers: A Review,” *Applied Sciences*, vol. 10, no. 18, p. 6614, Sep. 2020, doi: 10.3390/app10186614.

[75] Y. Yuan *et al.*, “A Fe3O4@Au-basedpseudo-homogeneous electrochemical immunosensor for AFP measurement using AFP antibody-GNPs-HRP as

detection probe," *Anal Biochem*, vol. 534, pp. 56–63, Oct. 2017, doi: 10.1016/j.ab.2017.07.015.

[76] H. Karimi-Maleh *et al.*, "A critical review on the use of potentiometric based biosensors for biomarkers detection," *Biosens Bioelectron*, vol. 184, p. 113252, Jul. 2021, doi: 10.1016/j.bios.2021.113252.

[77] J. Ding and W. Qin, "Recent advances in potentiometric biosensors," *TrAC Trends in Analytical Chemistry*, vol. 124, p. 115803, Mar. 2020, doi: 10.1016/j.trac.2019.115803.

[78] Z. Qiang *et al.*, "A new potentiometric immunosensor for determination of α-fetoprotein based on improved gelatin–silver complex film," *Electrochim Acta*, vol. 51, no. 18, pp. 3763–3768, May 2006, doi: 10.1016/j.electacta.2005.10.039.

[79] H.-W. Wang, C. Bringans, A. J. R. Hickey, J. A. Windsor, P. A. Kilmartin, and A. R. J. Phillips, "Cyclic Voltammetry in Biological Samples: A Systematic Review of Methods and Techniques Applicable to Clinical Settings," *Signals*, vol. 2, no. 1, pp. 138–158, Mar. 2021, doi: 10.3390/signals2010012.

[80] V. Periasamy *et al.*, "Novel same-metal three electrode system for cyclic voltammetry studies," *RSC Adv*, vol. 13, no. 9, pp. 5744–5752, 2023, doi: 10.1039/D3RA00457K.

[81] J. P.S. and D. S. Sutrave, "A Brief Study of Cyclic Voltammetry and Electrochemical Analysis," *Int J Chemtech Res*, vol. 11, no. 9, pp. 77–88, 2018, doi: 10.20902/IJCTR.2018.110911.

[82] S. Abdullah, S. Tonello, M. Borghetti, E. Sardini, and M. Serpelloni, "Potentiostats for Protein Biosensing: Design Considerations and Analysis on Measurement Characteristics," *J Sens*, vol. 2019, pp. 1–20, Mar. 2019, doi: 10.1155/2019/6729329.

[83] Hans J. Hansen, Zhengxing Qu, and David M. Goldenberg, "Alpha-fetoprotein Immu31 antibodies and fusion proteins and methods of use thereof," 2011

[84] A. Mosbah *et al.*, “Peptides Fixing Industrial Textile Dyes: A New Biochemical Method in Wastewater Treatment,” *J Chem*, vol. 2019, pp. 1–7, Jul. 2019, doi: 10.1155/2019/5081807.

[85] Innovagen AB, “PepCalc.com - Peptide property calculator.” Accessed: Jul. 17, 2024. [Online]. Available: https://pepcalc.com/

[86] K. Tripathi and J. D. Driskell, “Quantifying Bound and Active Antibodies Conjugated to Gold Nanoparticles: A Comprehensive and Robust Approach To Evaluate Immobilization Chemistry,” *ACS Omega*, vol. 3, no. 7, pp. 8253–8259, Jul. 2018, doi: 10.1021/acsomega.8b00591.

PUBLICATIONS FROM THE THESIS

Conference Papers

1. Gylyjov Muhammet, Gülyüz Sevgi, Yılmaz Özgür, Üstündağ Cem Bülent. (2024) Development of a Biosensor Surface for Liver Cancer Detection, ITU 3rd International Graduate Research Symposium (IGRS'24). Istanbul/Türkiye.